is only a few parts in a million, which is readily achieved for this liquid. High energy photons incident on the calorimeter face convert on the steel plates creating an electromagnetic shower which is absorbed by the following layers of steel and LA. The ionization created in each layer of argon allows one to sample the energy deposited by the shower as it develops. Since the entire shower is absorbed, the total ionization collected is proportional to the total energy of the shower. Such calorimeters have since become standard devices in high-energy experiments and similar instruments have been developed for hadron showers as well. A review of the calorimetric technique in general is given in [6.38].

Despite the many technical problems, the attractiveness of liquids has nevertheless led to proposals for more sophisticated detectors such as the liquid argon drift chamber [6.40] and the liquid argon TPC [6.41]. Because drift paths of a few tens of centimeters will be called for in these detectors, a purity level of less than 1 part in a billion will be necessary. Moreover, this purity must be maintained in the detector for long periods. This is to be contrasted to the LA calorimeter where purities of 1 ppm are generally used. Measurements of electron drift in a liquid argon [6.42] test chamber using a relatively simple purification system have been encouraging, however, yielding a purity of 0.2 ppb of oxygen equivalent and a measured extrapolated attenuation length of 7 m at an electric field strength of 1 kV/cm.

As a final remark, we note the relatively recent research into new ionization liquids. While LA can be purified to very high levels, the cryogenic system required proves to be cumbersome and constraining. For this reason, some physicists have begun searching for a suitable room-temperature liquid with the required drift properties and purity. Nonpolar organic liquids such as tetramethylsilane (TMS) or 2,2,4,4-tetramethylpentane (TMP) appear to show some of the desired properties and are now currently under investigation. A general review of the physics and chemistry of these liquids is given in [6.43].

7. Scintillation Detectors

The *scintillation* detector is undoubtedly one of the most often and widely used particle detection devices in nuclear and particle physics today. It makes use of the fact that certain materials when struck by a nuclear particle or radiation, emit a small flash of light, i.e. a scintillation. When coupled to an amplifying device such as a photomultiplier, these scintillations can be converted into electrical pulses which can then be analyzed and counted electronically to give information concerning the incident radiation.

Probably the earliest example of the use of scintillators for particle detection was the spinthariscope invented by Crookes in 1903. This instrument consisted of a ZnS screen which produced weak scintillations when struck by α-particles. When viewed by a microscope in a darkened room, they could be discerned with the naked eye, although some practice was necessary. It was tedious to use, therefore, and thus never very popular, even though it was spectacularly employed by Geiger and Marsden in their famous α scattering experiments. Indeed, with the invention of the gaseous ionization instruments, the optical scintillation counter fell into quick disuse.

In 1944, not quite a half century later, Curran and Baker resuscitated the instrument by replacing the human eye with the then newly developed photomultiplier tube. The weak scintillations could now be counted with an efficiency and reliability equal to that of the gaseous ionization instruments. Thus was born the modern electronic scintillation detector. New developments and improvements followed rapidly so that by the mid-1950's scintillation detectors were among the most reliable and convenient available. This is still true today. In this chapter, we will survey the existing materials and current techniques in use as well as describe their basic underlying principles.

7.1 General Characteristics

The basic elements of a scintillation detector are sketched below in Fig. 7.1. Generally, it consists of a scintillating material which is optically coupled to a photomultiplier either directly or via a light guide. As radiation passes through the scintillator, it excites the atoms and molecules making up the scintillator causing light to be emitted. This

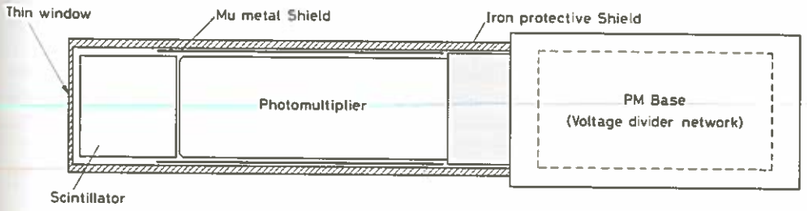

Fig. 7.1. Schematic diagram of a scintillation counter

light is transmitted to the photomultiplier (PM or PMT for short) where it is converted into a weak current of photoelectrons which is then further amplified by an electron-multiplier system. The resulting current signal is then analyzed by an electronics system.

In general, the scintillator signal is capable of providing a variety of information. Among its most outstanding features are:

1) *Sensitivity to Energy.* Above a certain minimum energy, most scintillators behave in a near linear fashion with respect to the energy deposited, i.e., the light output of a scintillator is directly proportional to the exciting energy. Since the photomultiplier is also a linear device, (when operated properly!), the amplitude of the final electrical signal will also be proportional to this energy. This makes the scintillator suitable as an energy spectrometer although it is not the ideal instrument for this purpose.
2) *Fast Time Response.* Scintillation detectors are fast instruments in the sense that their response and recovery times are short relative to other types of detectors. This faster response allows timing information, i.e., the time difference between two events, to be obtained with greater precision, for example. This and its fast recovery time also allow scintillation detectors to accept higher count rates since the dead time, i.e., the time that is lost while waiting for the scintillator to recover, is reduced.
3) *Pulse Shape Discrimination.* With certain scintillators, it is possible to distinguish between different types of particles by analyzing the shape of the emitted light pulses. This is due to the excitation of different fluorescence mechanisms by particles of different ionizing power. The technique is known as *pulse-shape discrimination* and is discussed in more detail later in this chapter.

Scintillator materials exhibit the property known as *luminescence*. Luminescent materials, when exposed to certain forms of energy, for example, light, heat, radiation, etc., absorb and reemit the energy in the form of visible light. If the reemission occurs immediately after absorption or more precisely within 10^{-8} s (10^{-8} s being roughly the time taken for atomic transitions), the process is usually called *fluorescence*. However, if reemission is delayed because the excited state is metastable, the process is called *phosphorescence* or *afterglow*. In such cases, the delay time between absorption and reemission may last anywhere from a few microseconds to hours depending on the material.

As a first approximation, the time evolution of the reemission process may be described as a simple exponential decay (Fig. 7.2)

$$N = \frac{N_0}{\tau_d} \exp\left(\frac{-t}{\tau_d}\right), \tag{7.1}$$

where N is the number of photons emitted at time t, N_0 the total number of photons emitted, and τ_d the decay constant. The finite rise time from zero to the maximum in most materials is usually much shorter than the decay time and has been taken as zero here for simplicity.

While this simple representation is adequate for most purposes, some, in fact, exhibit a more complex decay. A more accurate description, in these cases, may be given by a two-component exponential

$$N = A \exp\left(\frac{-t}{\tau_f}\right) + B \exp\left(\frac{-t}{\tau_s}\right), \tag{7.2}$$

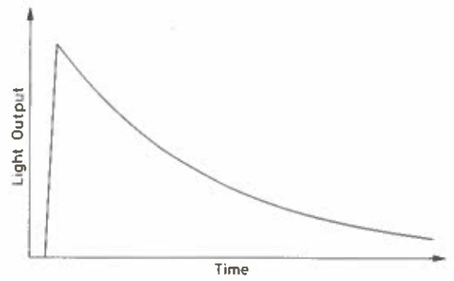

Fig. 7.2. Simple exponential decay of fluorescent radiation. The rise time is usually much faster than the decay time

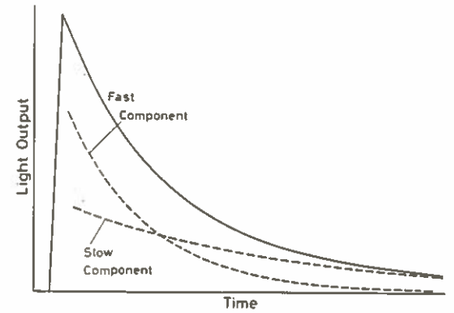

Fig. 7.3. Resolving scintillation light into *fast* (prompt) and *slow* (delayed) components. The *solid line* represents the total light decay curve

where τ_s and τ_f are the decay constants. For most scintillators, one component is generally much faster than the other so that it has become customary to refer to them as the *fast* and *slow* components (hence the subscripts f and s), or the *prompt* and *delayed* components. Their relative magnitudes, A and B, vary from material to material, although it is the fast component which generally dominates. Figure 7.3 shows the relation between these components. As will be seen in a later section, the existence of these two components forms the basis for the technique of pulse shape discrimination.

While many scintillating materials exist, not all are suitable as detectors. In general, a good detector scintillator should satisfy the following requirements:

1) high efficiency for conversion of exciting energy to fluorescent radiation
2) transparency to its fluorescent radiation so as to allow transmission of the light
3) emission in a spectral range consistent with the spectral response of existing photomultipliers
4) a short decay constant, τ.

At present, six types of scintillator materials are in use: organic crystals, organic liquids, plastics, inorganic crystals, gases and glasses. In the following sections we will briefly describe each category. Their basic properties are summarized in Table 7.1.

7.2 Organic Scintillators

The organic scintillators are aromatic hydrocarbon compounds containing linked or condensed benzene-ring structures. Their most distinguishing feature is a very rapid decay time on the order of a few nanoseconds or less.

Scintillation light in these compounds arises from transitions made by the *free* valence electrons of the molecules. These delocalized electrons are not associated with any particular atom in the molecule and occupy what are known as the *π-molecular orbitals*. A typical energy diagram for these orbitals is shown in Fig. 7.4, where we have distinguished the spin singlet states from the spin triplet states. The ground state is a singlet state which we denote by S_0. Above this level are the excited singlet states (S^*, S^{**}, ...) and the lowest triplet state (T_0) and its excited levels (T^*, T^{**}, ...). Also associat-

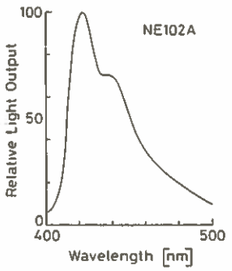

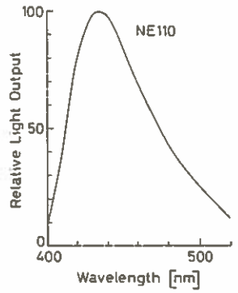

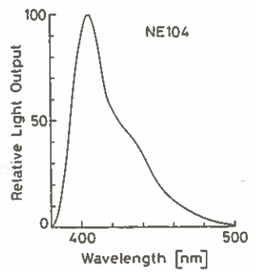

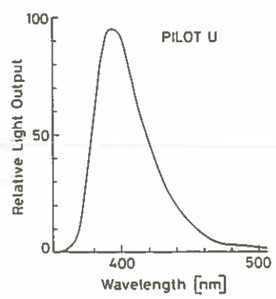

Fig. 7.5. Light emission spectra for several different plastic scintillators (from *Nuclear Enterprises* catalog [7.1])

this problem can be remedied to some extent by bubbling oxygen-free nitrogen through the liquid scintillator.

7.2.3 Plastics

In nuclear and particle physics, plastic scintillators are probably the most widely used of the organic detectors today. Like the organic liquids, plastic scintillators are also solutions of organic scintillators but in a solid plastic solvent. The most common and widely used plastics are polyvinyltoluene, polyphenylbenzene and polystyrene. Some common primary solutes are PBD, p-Terphenyl and PBO, which are dissolved in concentrations typically on the order of 10 g/l. Very often a secondary solute such as POPOP is also added for its wavelength shifting properties, but in a very much smaller proportion. The light emission spectra of several commercial plastics is shown in Fig. 7.5.

Plastics offer an extremely fast signal with a decay constant of about 2 – 3 ns and a high light output. Because of this fast decay, the finite rise time cannot be ignored in the description of the light pulse as was done in (7.1). The best mathematical description, as shown by *Bengston* and *Moszynski* [7.2], appears to be the convolution of a Gaussian with an exponential,

$$N(t) = N_0 f(\sigma, t) \exp\left(\frac{-t}{\tau}\right) , \tag{7.4}$$

where $f(\sigma, t)$ is a Gaussian with a standard deviation σ. Table 7.2 gives some fitted values of these parameters for a few common plastics.

Table 7.2. Gaussian and exponential parameters for light pulse description from several plastic scintillators (from *Bengston* and *Moszynski* [7.2])

Scintillator	σ [ns]	τ [ns]
NE102A	0.7	2.4
NE111	0.2	1.7
Naton 136	0.5	1.87

One of the major advantages of plastics is their flexibility. They are easily machined by normal means and shaped to desired forms. They are produced commercially in a wide variety of sizes and forms, ranging from thin films, a few $\mu g/cm^2$ thick, to large sheets, blocks and cylinders, and are relatively cheap. Moreover, various types of plastics are made offering differences in light transmission, speed, etc.

While they are generally quite rugged, plastics are easily attacked by organic solvents such as acetone and other aromatic compounds. They are, however, resistant to water pure methylal (dimethoxymethane), silicone grease and lower alcohols. When handling unprotected plastic, it is generally advisable to wear cotton or terylene gloves as the body acids from one's hands can cause a cracking of the plastic (often referred to as *craze*) after a period of time.

7.3 Inorganic Crystals

The inorganic scintillators are mainly crystals of alkali halides containing a small activator impurity. By far, the most commonly used material is NaI(Tl), where Thallium (Tl) is the impurity activator. Somewhat less common, but in active use is CsI(Tl), also with Tl as an impurity activator. Others crystals include CsF_2, CsI(Tl), CsI(Na), KI(Tl) and LiI(Eu). Among the non-alkali materials are $Bi_4Ge_3O_{12}$ (bismuth germanate or BGO), BaF_2, ZnS(Ag), ZnO(Ga), $CaWO_4$ and $CdWO_4$ among others (see Table 7.1).

The spectrum of emitted light from some of the more commonly used crystals is shown in Fig. 7.6. In general, inorganic scintillators are 2 – 3 orders of magnitude slower (~ 500 ns) in response than organic scintillators due to phosphorescence. (The one exception is CsF which has a decay time of 5 ns!) However, the time evolution of emission is, in most cases, well described by the simple one or two exponential decay forms.

A major disadvantage of certain inorganic crystals is hygroscopicity. NaI, in particular, is a prime example. To protect it from moisture in the air, it must be housed in an air tight protective enclosure. Other hygroscopic crystals are CsF, LiI(Eu) and KI(Tl). BGO and BaF_2, on the other hand, are non-hygroscopic and can be handled without protection, while CsI(Tl) is only slightly hygroscopic but can generally be handled without protection.

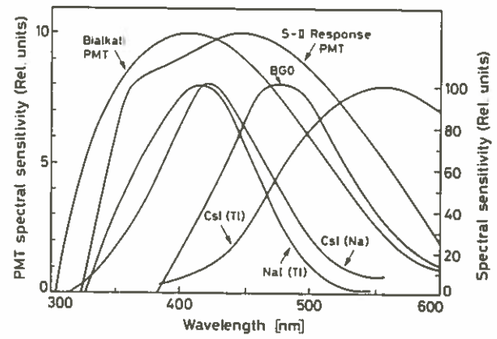

Fig. 7.6. Light emission spectra for different inorganic crystals (from *Harshaw Catalog* [7.3])

The advantage of inorganic crystals lies in their greater stopping power due to their higher density and higher atomic number. Among all the scintillators, they also have some of the highest light outputs, which results in better energy resolution. This makes them extremely suitable for the detection of gamma-rays and high-energy electrons and positrons.

While NaI has generally been the standard for these purposes, two new materials have recently drawn much attention from high-energy and nuclear physicists. These are $Bi_4Ge_3O_{12}$ (*Bismuth Germanate* or BGO) and BaF_2 (Barium Fluoride).

BGO is particularly interesting because of its very high-Z and greater efficiency for the photoelectric conversion of γ-rays. Relative to NaI, for example, it is 3 to 5 times more efficient and nonhygroscopic, as well. Its light output is lower than NaI, however, so that its resolution is about a factor two worse. Moreover, it is still relatively expensive and difficult to obtain in large quantities. Nevertheless, at very high energies it

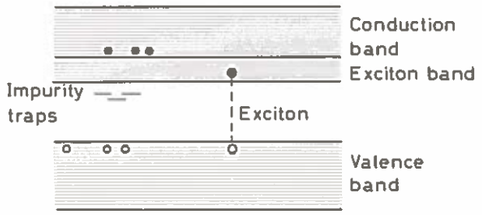

Fig. 7.7. Electronic band structure of inorganic crystals. Besides the formation of free electrons and holes, loosely coupled electron-hole pairs known as excitons are formed. Excitons can migrate through the crystal and be captured by impurity centers

presents an enormous advantage over NaI. BaF_2, on the other hand, has been discovered to have a very fast light component in the ultra-violet region. Decay times on the order of 500 ps have been measured in preliminary tests. This would make it twice as fast as the fastest plastics. The total light output of this component is low, however, and further development is necessary before its real usefulness can be determined.

Whereas the scintillation mechanism in organic materials is molecular in nature, that in inorganic scintillators is clearly characteristic of the electronic band structure found in crystals (see Fig. 7.7). When a nuclear particle enters the crystal, two principal processes can occur. It can ionize the crystal by exciting an electron from the valence band to the conduction band, creating a free electron and a free hole. Or it can create an *exciton* by exciting an electron to a band (the exciton band) located just below the conduction band. In this state the electron and hole remain bound together as a pair. However, the pair can move freely through the crystal. If the crystal now contains impurity atoms, electronic levels in the forbidden energy gap can be locally created. A migrating free hole or a hole from an exciton pair which encounters an impurity center, can then ionize the impurity atom. If now a subsequent electron arrives, it can fall into the opening left by the hole and make a transition from an excited state to the ground state, emitting radiation if such a deexcitation mode is allowed. If the transition is radiationless the impurity center becomes a *trap* and the energy is lost to other processes.

7.4 Gaseous Scintillators

These consist mainly of the noble gases: xenon, krypton, argon and helium, along with nitrogen. In these scintillators the atoms are individually excited and returned to their ground states within about 1 ns, so that their response is extremely rapid. However, the emitted light is generally in the ultraviolet, a wavelength region at which most photomultipliers are inefficient. One method of overcoming this difficulty has been to coat the walls of the container with a wavelength shifter such as diphenylstilbene (DPS). These materials strongly absorb light in the ultraviolet and emit in the blue-green region where photomultiplier cathodes are more efficient. In some cases, the PM windows are also coated with a thin layer of wavelength shifter as well.

Gas scintillators have generally been used in experiments with heavy charged particles or fission fragments. Here, mixtures of several gases (for example, 90% ^{3}He, 10% Xe) under pressures as high as 200 atm have been used to increase detection efficiency. In recent years, gas scintillators have been proposed as detectors in space physics as well.

Experiments have also been performed with solid and liquid xenon and liquid helium which have been found to scintillate.

7.5 Glasses

Glass scintillators are cerium activated lithium or boron silicates. However, boron glasses have light outputs some ten times lower than lithium so they are not very often employed today. Glass detectors are used primarily for neutron detection although they are also sensitive to β and γ radiation. They are most noteworthy for their resistance to all organic and inorganic reagents except for hydrofluoric acid. In addition, they have high melting points and are extremely resistant. These physical and chemical characteristics make them especially useful in extreme environmental conditions.

Their speed of response is between that of plastics and inorganic crystals, typically on the order of a few tens of nanoseconds. Light output, however, is low, never reaching more than 25 – 30% of that for anthracene.

For low-energy neutron detection, it is also possible to increase sensitivity by enriching the lithium component with ^{6}Li. Separation of neutron events from γ radiation events can then be made by using pulse height discrimination techniques.

7.6 Light Output Response

The light output of a scintillator refers more specifically to its efficiency for converting ionization energy to photons. This is an extremely important quantity, as it determines the efficiency and resolution of the scintillator. In general the light output is different for different types of particles at the same energy. Moreover, for a given particle type, it does not always vary linearly with energy.

As with ionization of gases, we can define an average energy loss required for the creation of a photon. Table 7.3 gives a brief list of this efficiency for several materials when electrons are the exciting particles. In general, this efficiency decreases for heavier particles. This behavior is seem in Fig. 7.8 for the case of plastic. Traditionally the light output of scintillators is referred to anthracene and is given as percent of anthracene light output. A more complete list of scintillator light outputs is given in Table 7.1.

It should be kept in mind that when considering the efficiency of a scintillation detector, the efficiency of the photomultiplier must also be taken into account, since they are inseparably coupled. A typical efficiency for the latter, as will be seen in the next chapter, is about 30%. Thus, assuming that all the emitted photons are collected, only 30% of these photons will ever be detected.

Table 7.3. Average energy loss per scintillator photon for electrons

Material	ε [eV/photon]
Anthracene	60
NaI	25
Plastic	100
BGO	300

8. Photomultipliers

Photomultipliers (PM's) are electron tube devices which convert light into a measurable electric current. They are extremely sensitive and, in nuclear and high-energy physics, are most often associated with scintillation detectors, although their uses are quite varied. It is nevertheless in this context that we will discuss the basic design and properties of photomultipliers, their characteristics under operation and some special techniques.

8.1 Basic Construction and Operation

Figure 8.1 shows a schematic diagram of a typical photomultiplier. It consists of a cathode made of photosensitive material followed by an electron collection system, an electron multiplier section (or dynode string as it is usually called) and finally an anode from which the final signal can be taken.[1] All parts are usually housed in an evacuated glass tube so that the whole photomultiplier has the appearance of an old-fashion electron tube.

During operation a high voltage is applied to the cathode, dynodes and anode such that a potential "*ladder*" is set up along the length of the cathode – dynode – anode structure. When an incident photon (from a scintillator for example) impinges upon the photocathode, an electron is emitted via the photoelectric effect. Because of the applied voltage, the electron is then directed and accelerated toward the first dynode, where upon striking, it transfers some of its energy to the electrons in the dynode. This causes secondary electrons to be emitted, which in turn, are accelerated towards the next dynode where more electrons are released and further accelerated. An electron cascade down the dynode string is thus created. At the anode, this cascade is collected to give a current which can be amplified and analyzed.

Photomultipliers may be operated in continuous mode, i.e., under a constant illumination, or in pulsed mode as is the case in scintillation counting. In either mode, if the cathode and dynode systems are assumed to be linear, the current at the output of the PM will be directly proportional to the number of incident photons. A radiation detector produced by coupling a scintillator to a PM (the scintillator produces photons in proportion to the energy deposited in the scintillator) would thus be capable of providing not only information on the particle's presence but also the energy it has left in the scintillator.

Let us now turn to a more detailed look at the various parts of the photomultiplier.

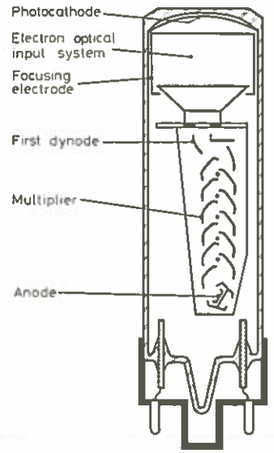

Fig. 8.1. Schematic diagram of a photomultiplier tube (from *Schonkeren* [9.1])

[1] An alternative structure rarely used with scintillation counters is the *side-on* PM. Here the photocathode is oriented so as to face the side of the tube rather than the end window. The dynode chain is then usually arranged in a circular fashion around the axis of the tube rather than linearly along it. The basic operating principle remains exactly the same, however.

8.2 The Photocathode

As we have seen, the photocathode converts incident light into a current of electrons by the photoelectric effect. To facilitate the passage of this light, the photosensitive material is deposited in a thin layer on the inside of the PM window which is usually made of glass or quartz. From Einstein's well-known formula,

$$E = h\nu - \phi \ , \tag{8.1}$$

where E is the kinetic energy of emitted electron, ν the frequency of incident light and ϕ the work function, it is clear that a certain minimum frequency is required before the photoelectric effect may take place. Above this threshold, however, the probability for this effect is far from being unity. Indeed, the efficiency for photoelectric conversion varies strongly with the frequency of the incident light and the structure of the material. This overall spectral response is expressed by the *quantum efficiency*, $\eta(\lambda)$,

$$\eta(\lambda) = \frac{\text{number of photoelectrons released}}{\text{number of incident photons on cathode } (\lambda)} \ , \tag{8.2}$$

where λ is the wavelength of the incident light. An equivalent quantity is the *radiant cathode sensitivity* which is defined as

$$S(\lambda) = \frac{I_k}{P(\lambda)} \ , \tag{8.3}$$

where I_k is the photoelectric emission current from the cathode and $P(\lambda)$ is the incident radiant power. The radiant cathode sensitivity is usually given in units of ampere/watts and is related to the quantum efficiency by

$$S(\lambda) = \lambda \eta(\lambda) \frac{e}{hc} \ . \tag{8.4}$$

For S in [A/W] and λ in nanometers

$$S(\lambda) = \frac{\lambda \eta(\lambda)}{1240} \ \text{[A/W]} \ . \tag{8.5}$$

A third unit is the *luminous cathode sensitivity* which is defined as the current per lumen of incident light flux. Since the lumen is essentially a physiological unit defined relative to the response of the human eye, the luminous sensitivity is not a unit to be recommended.

Figure 8.2 shows a graph of quantum efficiency vs λ for some of the more common photoelectric materials used in photomultipliers today. In general, the spectral response of these materials is such that only a certain band of wavelengths is efficiently converted. When choosing a PM, therefore, the primary consideration should be its sensitivity to the wavelength of the incident light. For the photocathodes shown in Fig. 8.2, the efficiency peaks near =400 nm, thereby making them quite suitable for use with scintillators. More than 50 other types of materials are in use, however, with spectral sensitivities varying from the infra-red to the ultraviolet. A brief list of the most

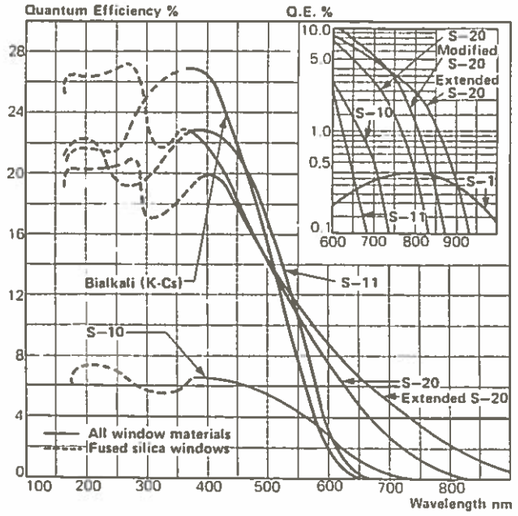

Fig. 8.2. Quantum efficiency of various photocathode materials (from *EMI Catalog* [8.2])

Table 8.1. Photocathode characteristics (from RTC catalog [8.3])

Cathode type	Composition	λ at peak response [nm]	Quantum efficiency at peak
S1 (C)	Ag–O–Cs	800	0.36
S4	SbCs	400	16
S11 (A)	SbCs	440	17
Super A	SbCs	440	22
S13 (U)	SbCs	440	17
S20 (T)	SbNa–KCs	420	20
S20R	SbNa–KCs	550	8
TU	SbNa–KCs	420	20
Bialkali	SbRb–Cs	420	26
Bialkali D	Sb–K–Cs	400	26
Bialkali DU	Sb–K–Cs	400	26
SB	Cs–Te	235	10

common types of photocathode is given in Table 8.1 along with their characteristics. Note that the different materials have been given standard type and code designations, an indication of their high frequency of use today.

Most of the photocathodes employed today are made of semiconductor materials formed from antimony plus one or more alkali metals. The choice of semiconductors rather than metals or other photoelectric substances lies in their much greater quantum efficiency for converting a photon to a *usable* electron. Indeed, in most metals, the quantum efficiency is not greater than 0.1% which means that an average of 1000 photons is needed to release one photoelectron. In contrast semiconductors have quantum efficiencies of the order of 10 to 30%, some two orders of magnitude higher! This difference is explained by their different intrinsic structures. Suppose, for example, an

electron absorbs a photon at some depth x in the material. In traveling to the surface, this electron will suffer an energy loss, $\Delta E = x(dE/dx)$, due to collisions with the atomic electrons along its path. In metals, these atomic electrons are essentially free so that large energy transfers result, i.e., the dE/dx is high. The probability of it reaching the surface with enough energy to overcome the potential barrier is therefore greatly reduced. This essentially restricts the usuable volume of the material to a very thin layer near the surface. The thickness of this layer is known as the *escape depth*. In contrast, semiconductors have an energy band structure with only a few electrons, those in the conduction and valence bands, being approximately free. The rest are tightly bound to the atoms. A photoelectron ejected from the conduction or valence band thus encounters less free electrons before reaching the surface. The only other possible collisions are with electrons bound to the lattice atoms. But due to the larger mass of the latter, little energy is transferred in these collisions. The photoelectron, therefore, is much more likely to reach the surface with a sufficient amount of energy to escape. The escape depth is thus much greater and the conversion efficiency higher.

A recent development in the construction of photocathodes has been the use of negative electron affinity materials such as gallium phosphide (GaP) heavily doped with zinc and a small quantity of cesium. In these materials the band structure near the surface is bent so that the bottom energy level of the conduction band is actually above the potential of the vacuum. The work function is thus negative. Without a potential barrier, then, an electron need only have enough energy to reach the surface in order to escape. Such materials, therefore, have greatly improved quantum efficiencies reaching as high as 80%! Unfortunately a number of problems still remain in constructing them as photocathodes so that only limited use has been made of them so far.

8.3 The Electron-Optical Input System

After emission from the photocathode, the electrons in the PM must be collected and focused onto the first stage of the electron multiplier section. This task is performed by the electron-optical input system. In most PM's, collection and focusing is accomplished through the application of an electric field in a suitable configuration. Magnetic fields or a combination of electric and magnetic fields may also be employed in principle, but their use is extremely rare. Figure 8.3 gives a schematic diagram of a typical electron-optical input system. Here an accelerating electrode at the same potential as the first dynode of the electron multiplier is used in conjunction with a focusing electrode placed on the side of the glass housing. Some lines of equipotential are shown along with some possible electron paths.

Regardless of the design, two important requirements must be met:

1) Collection must be as efficient as possible, i.e. as many emitted electrons as possible must reach the electron-multiplier section regardless of their point of origin on the cathode.
2) The time it takes for an emitted electron to travel from the cathode to the first dynode must be as independent as possible of the point of emission.

The second requirement is particularly important for *fast* photomultipliers which are used in timing experiments since it determines the time resolution of the detector. This is discussed further in Sect. 8.6.

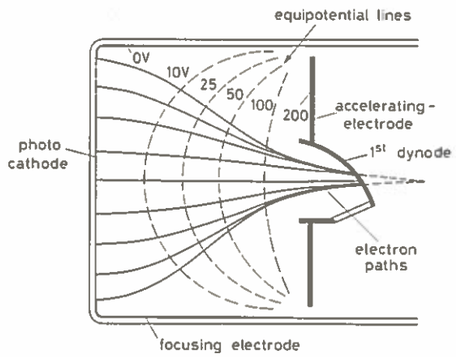

Fig. 8.3. Electron-optical input system of a typical *PM* (from *Schonkeren* [8.1])

8.4 The Electron-Multiplier Section

The electron-multiplier system amplifies the weak primary photocurrent by using a series of secondary emission electrodes or *dynodes* to produce a measurable current at the anode of the photomultiplier. The gain of each electrode is known as the *secondary emission factor, δ*. The theory of secondary electron emission is very similar to that described for photoelectric emission except that the photon is now replaced by an electron. On impact, energy is transferred directly to the electrons in the dynode material allowing a number of secondary electrons to escape. Since the conducting electrons in metals hinder this escape, as we have seen, it is not surprising that insulators and semiconductors are also used here as well.

One difference exists, however, in that a constant electric field must be maintained between the dynodes to accelerate and guide the electrons along the multiplier. Thus the secondary emission material must be deposited on a conducting material. A common procedure used today is to form an alloy of an alkali or alkaline earth metal with a more noble metal. During the mixing process, only the alkaline metal oxidizes, so that a thin insulating coating is formed on a conducting support. Materials in common use today are Ag – Mg, Cu – Be and Cs – Sb. These have varying advantages but all meet the requirements of a good dynode material:

1) high secondary emission factor, δ, i.e., the average number of secondary electrons emitted per primary electron;
2) stability of secondary emission effect under high currents;
3) low thermionic emission, i.e., low noise.

Most conventional PM's contain 10 to 14 stages, with total overall gains of up to 10^7 being obtained.

Like the photocathode, use has also been made of negative affinity materials as dynodes, in particular GaP. With this material the individual gain of each dynode is greatly increased so that the number of stages in a PM can be reduced. A 5-stage PM made of GaP dynodes, for example, would provide the same overall gain as a 14-stage

conventional PM. This reduction, as well, would diminish fluctuations in time as the path through which the cascade electrons must travel would also be much shorter.

8.4.1 Dynode Configurations

Dynode strings can be constructed in many ways and depending on the configuration, affect the response time and range of linearity of a photomultiplier. At present, five types of configurations are in use:

1) Venetian blind
2) Box and Grid
3) Linear focused
4) Circular focused (used in side-on PM's)
5) Microchannel plate.

The first four types are the more conventional structures and are illustrated in Fig. 8.4. In the Venetian blind configuration, the dynodes are wide strips of material placed

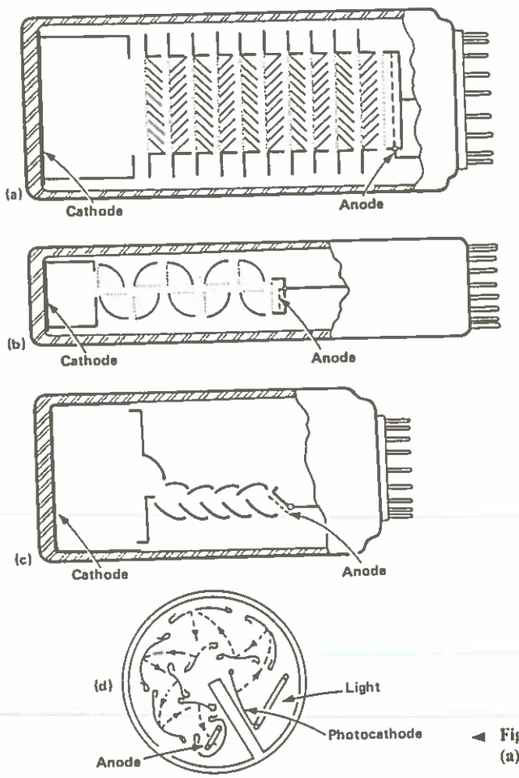

◄ **Fig. 8.4a–d.** Various dynode configurations for PM's (from *EMI Catalog* [8.2]): (a) venetian blind, (b) box and grid, (c) linear focused, (d) side-on configuration

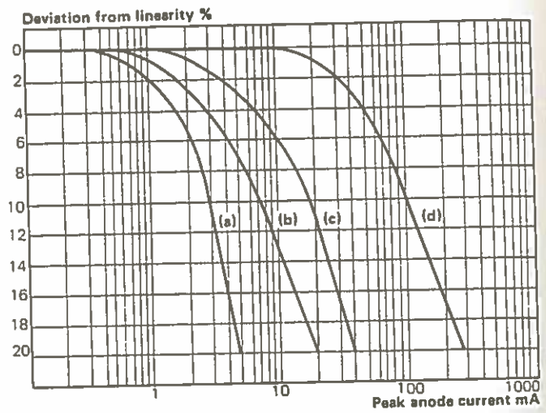

Fig. 8.5. Linearity of different dynode configurations: (*a*) box and grid, (*b*) venetian blind with standard voltage divider, (*c*) venetian blind with high current voltage divider, (*d*) linear focused with very high current divider (from *EMI Catalog* [8.2])

at an angle of 45 degrees with respect to the electron cascade axis. This is a simple system which offers a large input area to the incident primary electrons. The dynodes are easily placed in line and the dimensions are not critical. The disadvantage, however, is that it is impossible to prevent a fraction of the primary electrons from passing straight through. This results in a low gain and large variations in transit time. This is avoided in the box and grid, linear focused and circular types which reflect the electrons from one dynode to the next. Other inherent advantages of these latter types are that: (1) space is efficiently used, so that many dynodes can be used, and (2) the cathode and anode are well isolated, so that there is no risk of feedback.

The response linearity of the various types are compared in Fig. 8.5. From the point of view of overall performance, it is clear that the linear focused type is the more favorable of the four. However, the specific application must be considered. If linearity over a modest current range is desired, for example, a Venetian blind configuration would do just as well as a linear focused type and for a lower cost.

In recent years a new design has appeared which uses *microchannel plate multipliers*. This device, originally invented for use in image intensifiers, consists of a lead glass plate perforated by an array of microscopic channels (typically 10 – 100 μm in diameter) oriented parallel to each other (see Fig. 8.6). The inner surfaces of the channels are treated with a semiconductor material so as to act as secondary electron emitters while the flat end surfaces of the plate are coated with a metallic alloy so as to allow a potential difference to be applied along the length of the holes. Electrons entering a channel are thus accelerated along the hole until they eventually strike the wall to release further electrons which, in turn, are accelerated and so on. Each channel thus acts as a continuous dynode.

Typical microchannel plates have from $10^4 - 10^7$ holes and can provide multiplication factors of $10^3 - 10^4$. Two or three plates may also be cascaded to provide a higher overall gain. A common geometry is the *chevron* configuration shown in Fig. 8.7. Here

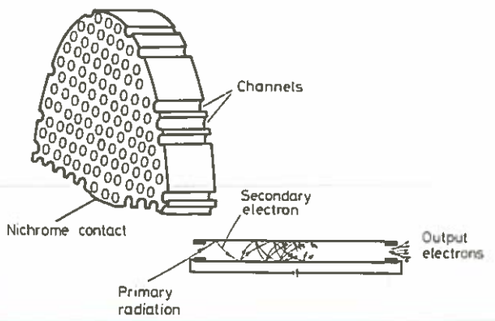

Fig. 8.6. Schematic diagram of a microchannel plate. The many channels act as continuous dynodes (from *Dhawan* [8.4]; picture © 1975 IEEE)

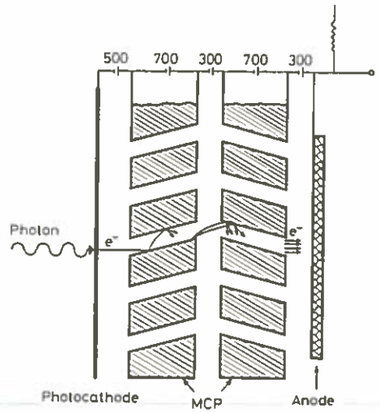

Fig. 8.7. Chevron configuration in a microchannel plate photomultiplier (after *Dhawan* [8.4]). A further increase in gain may be obtained by adding a third plate to form a "Z" configuration (picture © 1975 IEEE)

the channels are oriented at an angle with respect to the plate surfaces and to each other so as to avoid troublesome feedback from positive ions which occasionally form in the channels and drift backwards along the hole. The gain of the chevron configuration ranges from 10^5 to 10^7, which is comparable to the more conventional dynode structures. The advantage, however, is in the much improved timing properties due to the smaller dimensions of the microchannel plates. Transit times are only a few nanoseconds compared to a few tens of nanoseconds for the conventional types. This results in timing resolutions of ≤ 100 ps [8.4]. As well this smaller size makes microchannel plate PM's much less sensitive to magnetic fields. Tests, in fact, have shown, the immunity of these PM's to fields as high as 2 kG [8.4]. The disadvantages are high cost and their yet to be proven reliability. One particular problem which arises is that a cascade in one channel *drains* the neighboring channels for several μseconds [8.5] leading to nonlinearities for count rates above a few thousand per second.

8.4.2 Multiplier Response: The Single-Electron Spectrum

Ideally, the electron-multiplier system should provide a constant gain for all fixed energy electrons which enter the dynode system. In practice, this is not possible because of the statistical nature of the secondary emission process. Single electrons of the same energy entering the system will thus produce different numbers of secondary electrons, resulting in fluctuations in gain. This may be further amplified by variations in the secondary emission factor over the surface of the dynodes, differences in transit time, etc. A good measure of the extent of the fluctuations in a given multiplier chain is the *single electron spectrum*. This is the spectrum of PM output pulses resulting from the entry of single electrons only into the multiplier system. This distribution essentially gives the response of the electron-multiplier and can be measured by illuminating the PM with a very weak light source such that the probability of more than one single electron entering the multiplier at the same time is small. A more detailed description of the technique is given in the paper by *Hyman* et al. [8.6]. Because of the previously mentioned effects, the output pulse shapes will generally be different for each single-electron event. By integrating each current pulse, however, a new pulse whose amplitude is proportional to the total charge is obtained and thereby the gain for each event. Plotting each event versus gain then gives the response to the multiplier and thus the inherent gain fluctuations.

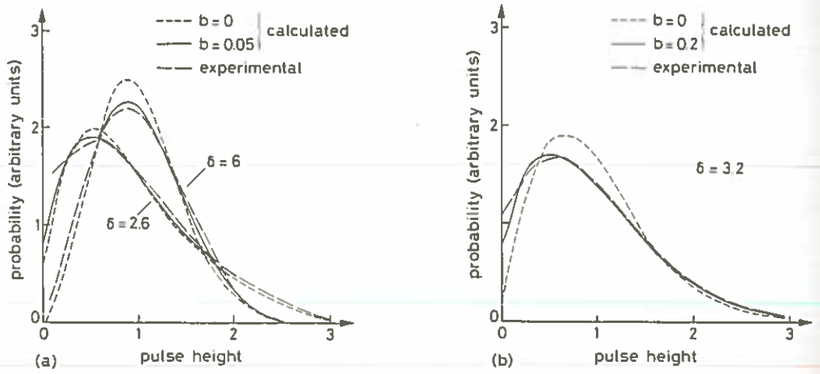

Fig. 8.8. Single-electron spectra for (a) linear-focused PM, (b) venetian blind PM (from *Schonkeren* [8.1])

Figure 8.8 illustrates some measured single-electron distributions for a linear-focused PM and a Venetian blind PM. Analytically, these spectra are best described by a *Polya* distribution (also called a *negative-binomial* distribution or *compound-Poisson* distribution). These are also shown in Fig. 8.8. The parameter b shown in Fig. 8.8 is the RMS deviation from perfect uniformity of the secondary emission factor over the surface of the dynode. As can be seen, the Venetian blind configuration is generally subject to more gain fluctuations than is the linear-focused type. This is due to better focused electrons in the latter which minimizes the effect of dynode nonuniformities.

8.5 Operating Parameters

8.5.1 Gain and Voltage Supply

The overall amplication factor or gain of a PM depends on the number of dynodes in the multiplier section and the secondary emission factor δ, which is a function of the energy of the primary electron. Figure 8.9 shows this dependence for several materials. In the multiplier chain, the energy of the electrons incident on each dynode is clearly a function of the potential difference, V_d, between the dynodes so that we can write

$$\delta = K V_\mathrm{d} \ , \tag{8.6}$$

where K is a proportionality constant. Assuming the applied voltage is equally divided among the dynodes, the overall gain of the PM is then

$$G = \delta^n = (K V_\mathrm{d})^n \ . \tag{8.7}$$

From (8.7) it is interesting to calculate the number of stages n, required for a fixed gain G with a minimum supply voltage V_b. Thus

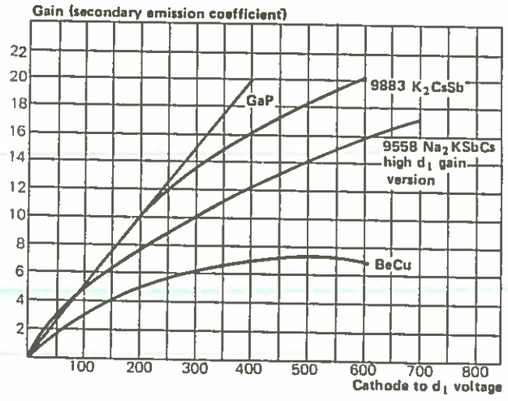

Fig. 8.9. Secondary emission factor for several dynode materials (from *EMI Catalog* [8.2])

$$V_b = nV_d = \frac{n}{K} G^{1/n} .$$

Minimizing, we find,

$$\frac{dV_b}{dn} = \frac{1}{K} G^{1/n} - \frac{n}{K} \frac{G^{1/n}}{n^2} \ln G = 0 , \quad n = \ln G \tag{8.8}$$

for operation at a minimum V_b. Apart from practical reasons, operating at the minimum voltage is desirable from the point of view of noise, etc. However, this comes into conflict with transit time spread and other factors (the number of pins, for example) which often results in the use of higher voltages.

An important relation which should be noted is the variation in gain with respect to supply voltage. From (8.7), we calculate

$$\frac{dG}{G} = n \frac{dV_d}{V_d} = n \frac{dV_b}{V_b} \tag{8.9}$$

which for $n = 10$ implies a 10% variation in gain for a 1% change in V_b! Thus, to maintain a gain stability of 1%, the voltage supply must be regulated to within 0.1%! Modern supply voltages are regulated to better than 0.05%.

8.5.2 Voltage Dividers

In the previous section we saw how crucial it is to have a well regulated voltage applied to the dynodes. Ideally, batteries would be the best stabilized voltage source, however the required number makes such a scheme impractical. The most common method is to use a stabilized high voltage supply in conjunction with a *voltage divider* (see Fig. 8.10). This system consists of a chain of resistances chosen such as to provide the desired voltage to each of the dynodes. Variable resistances can also be placed, for example, between the cathode and accelerating electrode, so as to allow a fine adjustment.

In designing such a divider, however, it is important to prevent the occurrence of large potential variations between the dynodes due to the changing currents in the tube. Such variations would cause changes in the overall gain and linearity of the PM. For this reason, it is important that the current in the resistance chain, known as the *bleeder* current, be large compared to the tube current. A calculation shows, in fact, that the variation in gain with anode current is

$$\frac{\Delta G}{G} = \frac{I_{an}}{I_{bl}} \frac{n(1-\delta)+1}{(n+1)(1-\delta)} , \tag{8.10}$$

with I_{an}: average anode current; I_{bl}: bleeder current; n: number of stages; δ: secondary emission factor.

To maintain a 1% linearity then, a bleeder current of about 100 times the average anode current would be necessary. In pulse mode operation, however, peak currents much larger than this current can still occur, particularly in the last few stages. To avoid momentary potential drops due to these peaks, the last stages can be maintained at a fixed potential by the addition of decoupling capacitors which provide the necessary charge during the peak period (see Fig. 8.10). These capacitors are then recharged

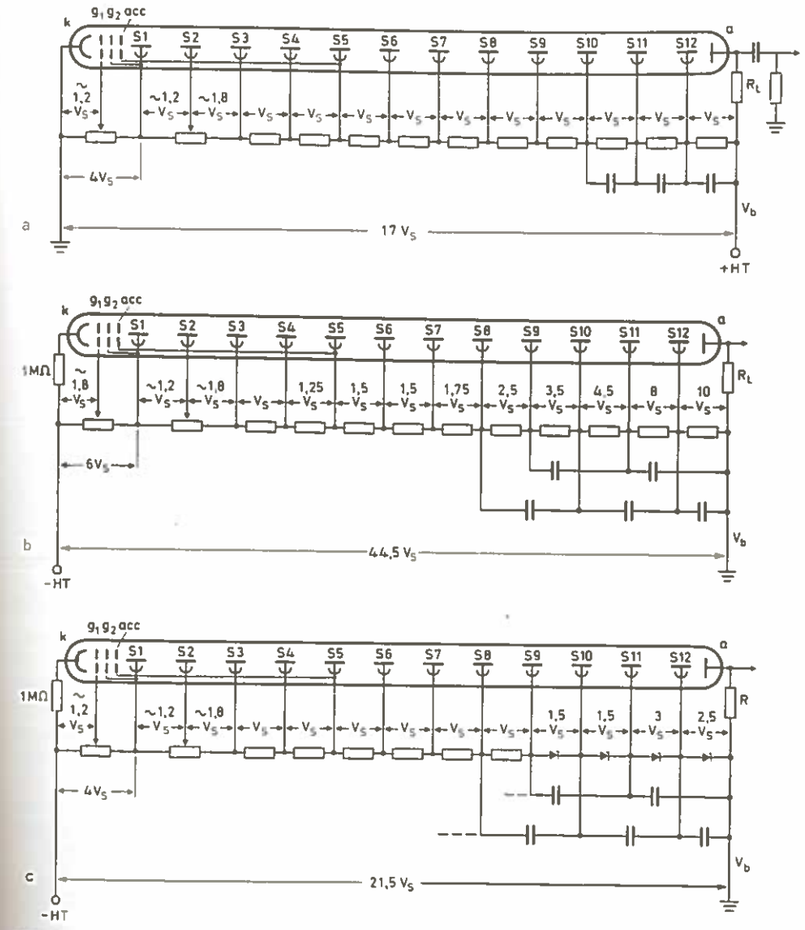

Fig. 8.10a–c. Examples of PM voltage divider networks (after examples from *Philips Catalog* [8.7]: (a) divider network using positive high voltage; note the AC coupling capacitor at the anode, (b) a network using negative high voltage and decoupling capacitors for maintaining the voltages between the last few dynodes, (c) example of the use of zener diodes to maintain voltages on the last few dynodes

during the non-peak periods. An alternate solution is to use Zener diodes in place of the resistances. These elements maintain a constant voltage for currents above a minimum threshold. In very high current applications, it may even be necessary to use a second external voltage supply to maintain the voltages on these last stages. Examples of the use of decoupling capacitors are shown in Fig. 8.10 (b) and (c).

The photomultiplier may be operated with either a positive or negative high voltage, as long as the potential of the dynodes is negative relative to the photocathode. If a pos-

itive high voltage is used, the photocathode should be kept at ground potential in order to avoid spurious discharges which might occur between the photocathode and the scintillator or outer envelope of the detector. Grounding the photocathode will also minimize noise from this component as well, an asset when doing pulse height spectroscopy. This advantage is somewhat offset, however, by the fact that the anode will be at constant positive potential. This requires that it be ac coupled through a capacitor in order to allow the pulse signal to pass at 0 dc level [see Fig. 8.10 (a)]. This is avoided if negative high voltage is used. The anode can then be kept at ground which allows it to be directly coupled to the detector electronics. For timing applications, this is particularly advantageous as the signal can be taken directly from the PM without suffering a reshaping (and thus loss of timing information) due to a coupling capacitor. The disadvantage, however, is that the cathode is now at a high negative potential. It thus becomes important to keep the glass well insulated so as to avoid leakage currents from the PM to the grounded material surrounding it.

8.5.3 Electrode Current. Linearity

The linearity of a PM depends strongly on the type of dynode configuration and the current in the tube. In general, photomultiplier linearity requires that the current at each stage be entirely collected by the following stage, so that a strict proportionality with the initial cathode current is maintained. Current collection, of course, depends on the voltage difference applied between stages. Figure 8.11, for example, shows the functional dependence of the cathode and anode currents on the applied voltages for various illuminations at the photocathode. These might be recognized as the Child-Langmuir characteristics for thermionic valves. At a given initial current, the current increases with applied voltage until a saturation level is reached where all the current is collected. The initial dependence on voltage is due to the formation of a space charge around the emitting electrode. This *cloud* of electrons tends to nullify the electric field in this region and prevents the acceleration of subsequently emitted electrons towards the receiving electrode.[2] As the voltage is increased, however, this space charge is swept

[2] This phenomena is referred to by some authors as *space charge saturation* which is often abbreviated to plain *saturation*. This should not be confused with the saturation of the Child-Langmuir characteristics!

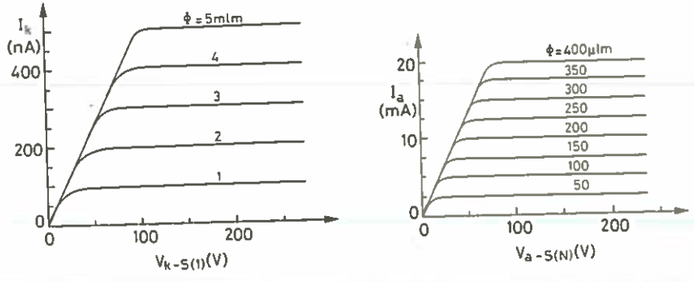

Fig. 8.11. Current-voltage characteristics of the PM cathode and anode under different illuminating light intensities (from *Schonkeren* [8.1])

away and all of the emitted current is collected. As a general rule, therefore, the cathode, dynode and anode currents should always be in the flat, saturated portion of the characteristic curve.

Maintaining these voltages during operation, however, requires more attention because of their dependence on the tube current. The resistivity of the photocathode, for example, is an important factor. This resistance is normally quite high, on the order of a few tenths of a MΩ or so. The emission of relatively small currents of photoelectrons can thus cause large changes in the potential of the photoemissive layer and a drop in its potential relative to the first dynode. This will, in turn, alter the collection efficiency. It is important, therefore, to work at a sufficiently high voltage so as to ensure staying on the flat part of the characteristic. This is also true for the dynodes, particularly the later stages where the current is high and the probability of space charge build-up is greater. To ensure linear operation, the distribution of voltage to these latter stages is generally increased over that of the earlier stages in most voltage dividers.

In the case of the anode, a similar effect occurs. Because it is connected in series to a load resistance (see Fig. 8.10), the anode voltage will fall as the anode current increases. Thus a change in the potential difference between the anode and the last dynode will occur. Since, the entire chain is kept at a constant voltage V_0, the potential differences between the earlier dynode stages will increase causing a change in gain and a loss of linearity. In order to stay on the saturated part of the characteristic, therefore, the current must be kept to within certain limiting values.

8.5.4 Pulse Shape

As we have seen, the output signal at the anode is a current or charge pulse whose total charge is proportional to the initial number of electrons emitted by the photocathode. In fact, more than any other device, the photomultiplier satisfies the requirements of an ideal current generator. As a circuit element, therefore, the PM may be equivalently represented [8.8] as a current generator in parallel with a resistance and capacitance (see Fig. 8.12). The resistance, R and the capacitance, C, here, represent the intrinsic resistance and capacitance of the anode plus those of any other elements which may be in the output circuit, e.g., the anode load resistor, cables, etc.

Let us examine the behavior of the signal at the circuit output. Assuming that the input is scintillator light described by an exponential decay, the current at the anode will be given by

$$I(t) = \frac{GNe}{\tau_s} \exp\left(\frac{-t}{\tau_s}\right), \tag{8.11}$$

with G: gain of PM; N: the number of photoelectrons emitted by the cathode; e: charge of the electron; τ_s: decay constant of scintillator.

We then have an equation of the form,

$$I(t) = \frac{V}{R} + C\frac{dV}{dt} \tag{8.12}$$

which has the solution

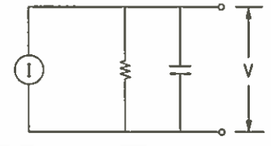

Fig. 8.12. Equivalent circuit for a photomultiplier. The PMT may be considered as an ideal current generator in parallel with a certain resistance and capacitance

11. Pulse Signals in Nuclear Electronics

As we have seen, modern detectors provide a variety of information on detected radiation in the form of electrical signals. In order to extract this information, however, the signal must be further processed by an electronics system. This system can be designed to perform an enormous variety of tasks. For example, it can be made to sort out the various signals from the detectors, extract energy information, determine the relative timing between two signals, etc., and based on this information, make a decision as to the acceptability of the event. It can then take appropriate action, for example, by activating a recording device. Indeed, many systems virtually run themselves!

In the following chapters, we will try to present an introduction to some of the logic and techniques of setting up an electronics system in nuclear and particle physics experiments and touch on some of the problems which will most likely be encountered. As will be seen, *nuclear electronics* today has been largely standardized into a modular form, i.e., the circuits for the basic processing functions (e.g., amplification, discrimination, etc.) have been built into separate electronic modules of standard mechanical and electrical specifications which are then interconnected as desired. These systems, (NIM, CAMAC), which we will discuss later, are extremely advantageous as they allow the design of many different systems using the same set of modules. Moreover, since the physical and electrical specifications have been standardized and accepted throughout the world, modules from different laboratories can be freely exchanged without any problem in compatibility. An analogous example, perhaps more familiar to the reader, is the modern Hi-Fi system. While the various components (e.g. amplifier, tuner, tape deck, etc.) are constructed separately by many different manufacturers, they are all compatible with each other so that a variety of Hi-Fi systems can be created with no problem.

In both cases, as well, a detailed knowledge of electronics at the level of circuit design is not necessary in order to set up the system, only an understanding of the logic. In the following chapters, therefore, we will assume only an elementary knowledge of circuits and give explanations where some more sophisticated knowledge is needed.

We begin in this chapter with a discussion of pulse signals and their characteristics.

11.1 Pulse Signal Terminology

The coding of information in nuclear electronics is generally done in the form of pulse signals. These are brief surges of current or voltage in which information may be contained in one or more of its characteristics, for example, its polarity, amplitude, shape, its occurrence in time relative to another pulse, or simply its mere presence. This mode of coding, as opposed to other systems, for example, amplitude or frequency modulation of a sinusoidal signal, is natural in nuclear and particle physics, for, as we have

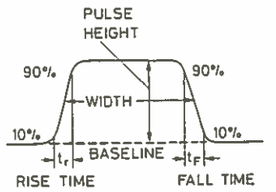

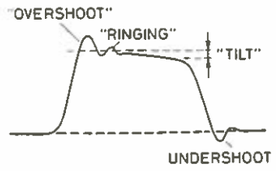

Fig. 11.1. Pulse signal terminology

seen most modern particle detectors are pulse devices. To begin our discussion, let us first identify some basic characteristics of pulse signals and define the terms which are associated with these features. Figure 11.1 (a) shows an ideal rectangular pulse, either in voltage or current, as a function of time. In nuclear electronics, this time scale may vary from micro-seconds to fractions of a nanosecond. We can define the following features:

1) *Baseline.* The baseline of the signal is the voltage or current level to which the pulse decays. While this is usually zero, it is possible for the baseline to be at some other level due to the superimposition of a constant dc voltage or current, or to fluctuations in the pulse shape, count rate etc.
2) *Pulse Height or Amplitude.* The amplitude is the height of the pulse as measured from its maximum value to the instantaneous baseline below this peak.
3) *Signal Width.* This is the full width of the signal usually taken at the half-maximum of the signal (FWHM).
4) *Leading Edge.* The leading edge is that flank of the signal which comes first in time.
5) *Falling Edge.* The falling edge or tail is that flank which is last in time.
6) *Rise Time.* This is the time it takes for the pulse to rise from 10 to 90% of its full amplitude. The rise time essentially determines the rapidity of the signal and is extremely important for timing applications.
7) *Fall Time.* In analogy with rise time, the fall time is the time it takes for the signal to fall from 90 to 10% of its full amplitude.
8) *Unipolar and Bipolar.* Signal pulses may also be unipolar or bipolar. A unipolar pulse is one which has one major lobe entirely (excepting a small possible undershoot) on one side of the baseline. In contrast, bipolar pulses cross the baseline and form a second major lobe of opposite polarity. Figure 11.2 illustrates these two types. Both are used in nuclear electronics.

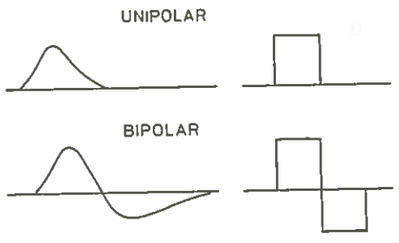

Fig. 11.2. Unipolar and bipolar pulses

In practice, however, it will be found that pulses are very often distorted by various factors in the circuit. Figure 11.1 also illustrates some of various deviations in form which may be observed and the terminology which is used to describe the effects.

11.2 Analog and Digital Signals

Pulse signals, and signals in general, carry information in two forms: *analog* or *digital*. An analog signal codes continuously-valued information by varying one or more of its characteristics, (e.g. amplitude and/or shape), in some fixed relation to the information value. The voltage signal from a microphone, for example, *analogically* varies its amplitude continuously in proportion to the intensity of the sound it picks up. Similarly, a scintillation detector, as we have seen, generates pulses whose amplitudes are in proportion to the energy deposited in the detector. If a beam of particles with a continuous spectrum of energies is allowed to strike the detector, then a continuous analog spectrum of pulse heights will result. More generally, if we consider each possible amplitude or shape of a pulse as a *state*, then the analog signal can be said to have an infinite, noncountable number of states. In nuclear physics, most analog pulses are of the amplitude varying type, although in certain cases, such as pulse shape discrimination, information is also contained in the shape of the pulse. Since the proportionality between pulse height and energy is usually linear, these pulses are also referred to as *linear* pulses.

In contrast to the continuum of amplitudes or shapes which are possible for the analog pulse, the *digital* or *logic* signal may only take on a discrete number of states; the information represented is thus of a *quantized* nature. For example, the signal from a Geiger-Müller counter has essentially two states: present or not present.[1] The corresponding information is then simply: *yes*, radiation was detected, or *no*, radiation was not detected. No finer distinction is possible. Similarly, we might imagine a ten-state rectangular signal which can only take on the amplitudes 0, 1, 2, 3, ... 9 V, for example. Such a signal might then be used to represent the decimal integers from 0 to 9, only. Technically, however, it is difficult to find electrical devices which have more than two naturally quantized states. In practice, therefore, all logic signals are limited to two-states only. When reference is made to logic or digital signals, therefore, this generally implies the two-state variety.

Although in a certain sense, the logic signal carries *less* information than the analog signal, from a technical point of view it is the more reliable since the exact amplitude or form of the signal need not be perfectly preserved. Indeed, distortion or noise, which are always present in any circuit, will easily alter the information in an analog signal but would have much less effect on the determination of what state a logic signal is in. Moreover, the limited information-carrying ability of the logic signal may be overcome by using several logic signals to represent equivalent analog information in numerical form, that is, each logic signal would represent a digit in a number (hence the name *digital* signal) whose value corresponds to the analog information. Since only two states are available, this number must be in the binary system. One logic state, for example, *pulse-present* would represent the binary digit *1*, while the other state *pulse-absent* would represent *0*. The contrary, of course, would also be an equally valid system, as would a system involving positive and negative signals, etc. The important point is to keep the same convention throughout. An entire binary number would then consist of a string of logic signals, which could be transmitted serially, i.e., one after the other, or simultaneously along an equal number of parallel lines. This involves, of course, more signals and electronics, however, with the advent of miniaturization and large scale integrated electronics, this disadvantage is removed giving digital systems a clear superiority over analog systems.

In nuclear electronics, the two electrical states of the logic signal are standardized by the NIM convention. One logic state is usually taken as 0 V, i.e., no pulse at all, and the other at a fixed voltage level. Because of the obvious difficulty in generating a pulse

[1] Recall that the Geiger counter signal is saturated so that when it is present, it has the same amplitude and shape regardless of the energy of the radiation detected.

with exactly the right voltage level, a band of voltages into which the signal must fall is defined instead. These limits are given in the next chapter. As a general rule, the analog signals from radiation detectors are changed into logic signals at sometime or another in a nuclear electronics chain. Usually this is performed relatively early after analyzing the detector signal for certain conditions, for example, a certain minimum energy. Here, the detector signal is passed through a *discriminator* which tests the amplitude of the signal for the minimum height. If *yes*, a logic signal is issued, if *no*, no signal (i.e., logic state *no*) is issued. This signal may then be fed into other modules for processing, and depending on the outcome, may initiate further operations: for example, incrementing a counting device or starting a timer, etc. In spectroscopy measurements, where the analog signal is to be analyzed for the exact value of its amplitude, the signal is often *digitized* and the numerical result treated with a computer. Electronic devices which perform such a conversion are know as *analog-to-digital converters* (ADC's). In a similar manner, a digital signal may be converted into an analog signal by a *digital-to-analog converter* (DAC).

As will be seen in Chap. 14, a variety of electronic modules exist for signal processing, some treating analog signals only, others logic signals only, and some converting the two. We emphasize here the importance of distinguishing between the different types. Sending a logic signal into a module expecting an analog pulse or vice-versa does no harm generally, however, unless there is a specific reason for doing so, the result is meaningless.

11.3 Fast and Slow Signals

For technical reasons which we will consider later, it is important to distinguish between *fast* and *slow* pulses in an electronics system. *Fast* signals generally refer to pulses with rise times of a few nanoseconds or *less* while *slow* signals have rise times on the order of hundreds of nanosecond or *greater*. This definition includes both linear and logic signals.

Fast pulses are very important for timing applications and high count rates; in these applications it is very important to preserve their rapid rise times throughout the electronics system. Slow pulses, on the other hand, are generally less susceptible to noise and offer better pulse height information for spectroscopy work.

While it would certainly be more convenient to be able to work with both these types in an identical manner, fast signals, unfortunately, must be treated differently from slow pulses. This is because of their much greater susceptibility to distortion from small, stray capacitances, inductances and resistances in the circuits and interconnections. These elements can combine to form inadvertent, *parasitic* circuits; for example, equivalent RC or RL circuits which have fast transient responses due to the small values of R, C and L (recall that the time constant of the RC circuit is $\tau = RC$). Compared to slow signals these transients are negligibly short. Compared to fast signals, however, these transients are of the same order of magnitude in duration. A fast signal passing through one of these inadvertent circuits can thus be quickly deformed.

A second problem, which will be treated in Chap. 13, is distortion from reflections in the interconnecting cables. This arises because of the short duration of fast pulses relative to their time of transit in the interconnection. Processing fast signals, therefore, not only requires special attention in the circuit design but also in the interconnections between modules. For this reason, essentially two standardized NIM systems have arisen: one designed for fast nanosecond pulses and the other for slower pulses. Within each system the electronic modules are compatible with each other; however, mixing the two without proper adaptation will invariably lead to problems. And, as already mentioned, special attention must be paid to how the interconnections are made in fast systems. This is one of the most important points to keep in mind when setting up nuclear electronics.

11.4 The Frequency Domain. Bandwidth

Our description and visualization of pulses so far has been in terms of its variation in time. A complete understanding of pulse electronics, especially pulse distortion, however, also requires viewing the pulse in terms of its frequency components. From Fourier analysis, it is well known that a pulse form can be decomposed into a superposition of many pure sinusoidal frequencies. Indeed, if we have a pulse whose shape in time is represented by the function $f(t)$, where t is time, then it may be decomposed as

$$f(t) = \frac{1}{\sqrt{2\pi}} \int_{-\infty}^{\infty} g(\omega) \exp(i\omega t)\, d\omega \ , \tag{11.1}$$

where $g(\omega)$ is the *Fourier transform* or frequency spectrum of the pulse. Inverting (11.1) gives

$$g(\omega) = \frac{1}{\sqrt{2\pi}} \int_{-\infty}^{\infty} f(t) \exp(-i\omega t)\, dt \ . \tag{11.2}$$

As a representative example, consider an ideal rectangular pulse of width T shown in Fig. 11.3. For simplicity, we have taken the pulse to be centered at $t = 0$. Thus,

$$f(t) = \begin{cases} A & |t| < T/2 \\ 0 & |t| > T/2 \ . \end{cases} \tag{11.3}$$

If we Fourier analyze this function, we find the spectrum

$$g(\omega) = \frac{1}{\sqrt{2\pi}} \int A \exp(-i\omega t)\, dt = \frac{AT}{\sqrt{2\pi}} \frac{\sin(\omega T/2)}{(\omega T/2)} \ , \tag{11.4}$$

which is plotted in Fig. 11.3 as a function of frequency $f = \omega/2\pi$. As can be seen, $f(t)$ contains a continuous spectrum of frequency components from 0 to ∞, arranged in a band structure reminiscent of optical diffraction. The energy or power contained in each frequency component is the square of $g(\omega)$:

$$E(\omega) = |g(\omega)|^2 \ . \tag{11.5}$$

The negative frequencies are, of course, purely imaginary.

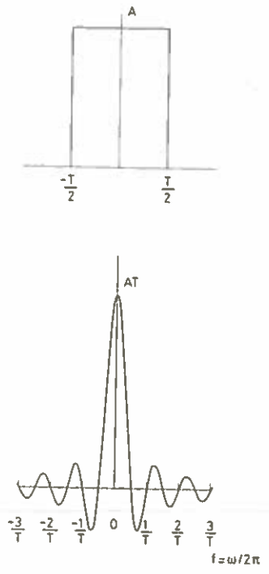

Fig. 11.3. Fourier spectrum of a rectangular pulse

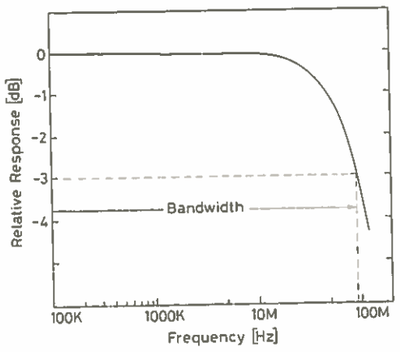

Fig. 11.4. Typical frequency response curve. The frequency range between the points at which the curve falls by 3 dB from its maximum value is defined as the response bandwidth. The lower end of the band is not seen on this graph

All frequencies play a role in the shaping of the function $f(t)$. Thus, in order for an electronic device to faithfully treat the information contained in this signal, the device must be capable of responding uniformly to an infinite range of frequencies. In any real circuit, of course, this is impossible. There will always be resistive and reactive components present, which will filter out some frequencies more than others, so that the response is limited to a finite range in ω. This is also true for the interconnecting cables, as will be seen later. Figure 11.4 shows a typical response curve. The range of frequencies delimited by the points at which the response falls by 3 dB is defined as the *bandwidth* and represents the range of accepted frequencies. Frequencies outside this range are attenuated or cutoff.

While complete and faithful signal reproduction is desirable, it is of course not absolutely necessary that this be ideally so. Indeed, what is important is that those parts of the signal carrying information be reproduced with good fidelity. For nuclear pulses, these parts are the amplitude and, more particularly, the fast rising edge. To investigate the effect of bandwidth on these characteristics, Fig. 11.5 shows the resulting pulse shapes obtained by integrating (11.4) from $f = 0$ to various cut-off frequencies.

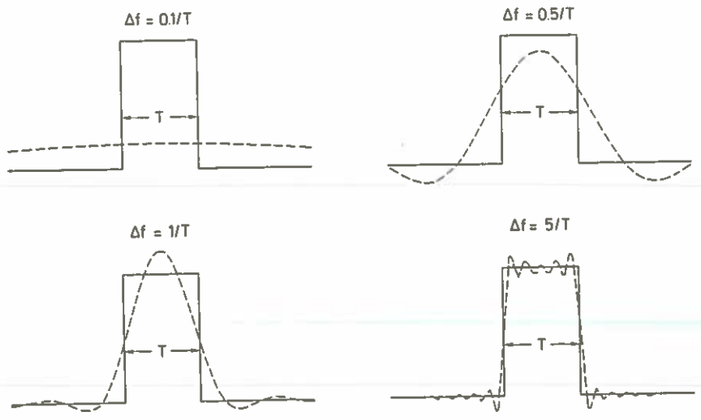

Fig. 11.5. Effect of limited bandwidth on a rectangular pulse

As can be seen, a minimum bandwidth of $\Delta f \geq 1/T$, is necessary to give a reasonable approximation of the pulse. This is not too surprising as most of the frequencies are contained in this region as seen in Fig. 11.3. Moreover, by comparing the various figures, it can be seen that the high frequency components allow the signal to rise sharply, while the lower frequencies account for the flat parts. For a typical fast pulse of say 5 ns width this would mean $\Delta f \geq 200$ MHz. For slow pulses, this limit, of course, is lower. Fast nuclear electronics, therefore, must be capable of accepting frequencies up to $\simeq$500 MHz. In addition, we can also define a lower limit. Since we are only interested in the fast rising edge and not the flat parts, eliminating some of the lower frequencies should not affect the information in our signal too much either. For nanosecond pulses, it can be shown, in fact, that frequencies up to $\simeq$100 kHz can be removed with no harm. As a practical rule, therefore, only the frequencies between $\simeq$100 kHz and $\simeq$ several hundred MHz to 1 GHz are of importance in nuclear electronics. As we will see in a later chapter, achieving a few hundred MHz bandwidth is not a simple task.

12. The NIM Standard

The first (and simplest) standard established for nuclear and high energy physics is a modular system called *NIM (Nuclear Instrument Module)*. In this system, the basic electronic apparatus, for example, amplifiers, discriminators, etc., are constructed in the form of modules according to standard mechanical and electrical specifications. These modules, in turn, fit into standardized *bins* which supply the modules with standard power voltages. Any NIM module will fit into any NIM bin. A specific electronic system for a given application can easily be created, then, by simply collecting the necessary modules, (e.g. an amplifier, a discriminator and a scaler for a simple counting system), installing them in a NIM bin and cabling them accordingly. After the experiment, the modules can be transferred to another NIM system, for example, or rearranged and/or combined with other modules for another application, or stored for later use. The NIM system offers enormous advantages in flexibility, interchange of instruments, reduced design effort, ease in updating instruments, etc. – all of which leads to reduced costs and more efficient use of instruments. For this reason the NIM system is now adopted worldwide by research laboratories and commercial enterprises.

12.1 Modules

Mechanically, NIM modules must have a minimum standard width of 1.35 inches (3.43 cm) and a height of 8.75 in (22.225 cm). They can, however, also be built in multiples of this standard, that is, double-width, triple-width, etc. Figure 12.1 shows an

Fig. 12.1. NIM modules

example of single and double width modules. Power for these modules is supplied through a rear connector which fits into a corresponding connector in the bin. Apart from these mechanical restrictions and the power voltages to be described below, however, the individual is free to design his module in any way desired, thus allowing for new developments and improvements.

12.2 Power Bins

The standard NIM bin is constructed to accept up to 12 single-width modules or a lesser number of multiple-width modules. Figure 12.2 shows a typical example. The external bin dimensions are such as to allow mounting in 19-inch racks or cabinets. The rear power connectors must provide, at the very least, four standard dc voltages, -12 V, $+12$ V, -24 V and $+24$ V, as designated by the NIM convention. However, many bins also provide -6 V and $+6$ V. Prior to 1966, these voltages were not officially part of the NIM standard, but in the past decade their use has become so increasingly common that they are essentially standard now.

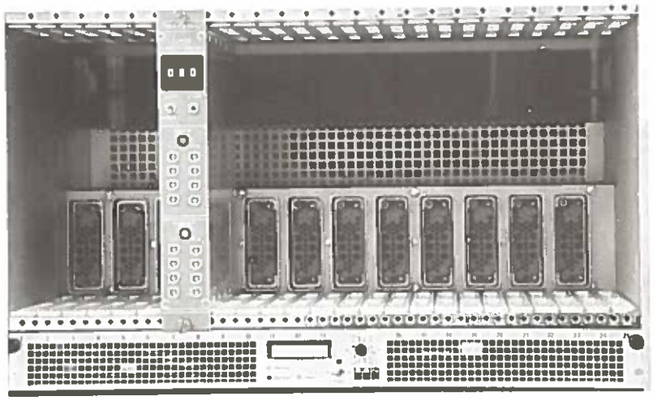

Fig. 12.2
A NIM bin

The pin assignments of the rear connectors are shown in Fig. 12.3. All pins are bussed to all of the 12 rear connectors, that is, all #10 pins, for example, are connected to a common conductor, as are all #11 pins, etc. However, since only the standard pins (marked with an asterisk) are used, manufacturers have tended to bus these pins only, so as to discourage use of the others. In any case, pins marked as *reserved* are not to be used since the NIM committee retains these as options for possible use at a later date. Pins marked as *spare* can be used as desired by the individual.

12.3 NIM Logic Signals

NIM modules include both analog and digital instruments. It should be recalled that in analog signals, information is carried in the amplitude or shape of the signal, thus they

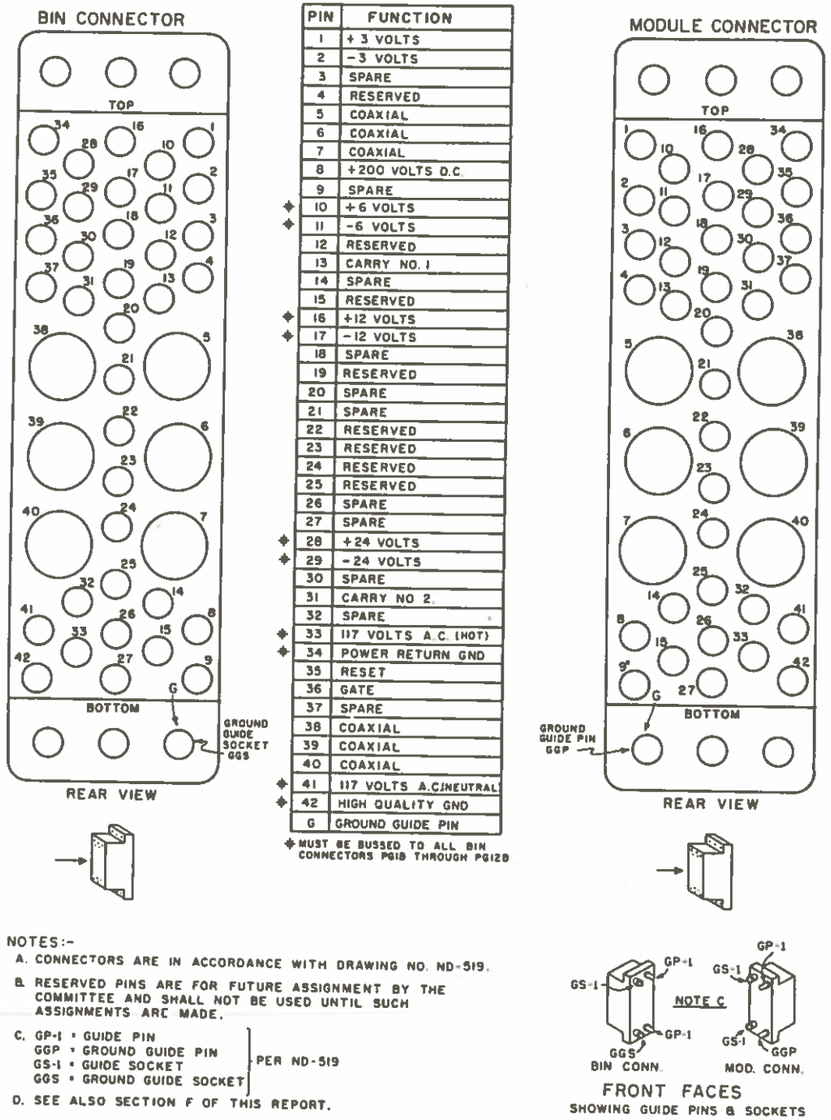

PIN	FUNCTION
1	+3 VOLTS
2	−3 VOLTS
3	SPARE
4	RESERVED
5	COAXIAL
6	COAXIAL
7	COAXIAL
8	+200 VOLTS D.C.
9	SPARE
✦ 10	+6 VOLTS
✦ 11	−6 VOLTS
12	RESERVED
13	CARRY NO. 1
14	SPARE
15	RESERVED
✦ 16	+12 VOLTS
✦ 17	−12 VOLTS
18	SPARE
19	RESERVED
20	SPARE
21	SPARE
22	RESERVED
23	RESERVED
24	RESERVED
25	RESERVED
26	SPARE
27	SPARE
✦ 28	+24 VOLTS
✦ 29	−24 VOLTS
30	SPARE
31	CARRY NO 2.
32	SPARE
✦ 33	117 VOLTS A.C. (HOT)
✦ 34	POWER RETURN GND
35	RESET
36	GATE
37	SPARE
38	COAXIAL
39	COAXIAL
40	COAXIAL
✦ 41	117 VOLTS A.C.NEUTRAL
✦ 42	HIGH QUALITY GND
G	GROUND GUIDE PIN

✦ MUST BE BUSSED TO ALL BIN CONNECTORS PGIB THROUGH PGI2B

Fig. 12.3. Pin assignments on a NIM rear connector (from *Costrell* [12.1])

are of continuously varying heights and form. Digital or logic signals, on the other hand, are of fixed shape and have only two possible states: *yes* or *no*. It is customary to refer to the two states as *logical 0* and *logical 1*; which signal is chosen as *1* or *0* is arbitrary however. For example, one might designate a +5 V signal as *logical 1* and 0 V as *logical 0* or equally, a −5 V signal as *1* and −1 V as *0*. Such a signal might then be used to indicate the presence or absence of a particle in a detector, for example. Thus, it can be used to increment a scaler or to form a coincidence with another signal, etc. This, of course, requires that the scaler or coincidence unit recognize the signals. In practice, a voltage range into which the logic signal must fall is defined rather than a definite level. This allows for fluctuations in the signal due to noise or interference, etc.

While it is not an official part of the NIM convention, an essential standardization has also been set for the voltage levels of logic signals. These levels have been designated as *Preferred Practice* and are generally accepted by manufacturers and laboratories.

Two types of standards exist: *slow-positive* logic and *fast-negative* logic. The first refers to signals of relatively slow rise time, on the order of hundreds of nanoseconds or more. They are of positive polarity and are used with slow detector systems. Table 12.1 defines the voltage levels for this logic. Note that the definition is in terms of a voltage across a 1000 Ω impedance. This implies that the current carried by the signal is very small. The consequence of this is that slow-positive signals cannot be transmitted through long cables. As we will see in the next chapter, the characteristic impedance of most cables is not more than about 100 Ω. After a meter or two of cable, therefore, the signal becomes highly attenuated.

Table 12.1. Slow-positive NIM logic

	Output must deliver	Input must accept
Logic 1	+4 to +12 V	+3 to +12 V
Logic 0	+1 to −2 V	+1.5 to −2 V

Input impedance must be 1000 Ω or more
Source impedance 10 Ω or less

Fast-negative logic, often referred to as *NIM logic*, employs extremely fast signals with rise times on the order of 1 ns and comparable widths. This type is often used in experiments using fast plastic counters (in high-energy physics, for example) where high count rates or fast timing is desired. The NIM logic levels are defined in Table 12.2. Note that unlike slow-positive logic, the definition is current based rather than voltage based. As well, the input and output impedances of all fast NIM modules are

Table 12.2. Fast-negative NIM logic

	Output must deliver	Input must accept
Logic 1	−14 mA to −18 mA	−12 mA to −36 mA
Logic 0	−1 mA to +1 mA	−4 mA to +20 mA

Current into 50 Ω
Neither risetime nor width is defined

required to be 50 Ω, as are the characteristic impedances of the connecting cables. The corresponding voltage levels are thus 0 V and −0.8 V for logic *0* and *1* respectively. In contrast to slow positive signals, the fast NIM-signals can be transmitted through relatively long lengths of cable.

12.4 TTL and ECL Logic Signals

While not part of the NIM standard two other logic families are often found in nuclear and particle physics electronics. The first is the *TTL* (Transistor-Transistor Logic) logic family. This is a positive going logic which is very often found on NIM electronics modules. The levels are defined in Table 12.3.

The second is a logic family which is becoming increasingly popular in high-energy physics. This is the *emitter-coupled* logic (ECL) family which is currently the fastest form of digital logic available. These levels are also defined in Table 12.3.

Table 12.3. TTL and ECL signal levels

	TTL	ECL
Logic 1	2−5V	−1.75 V
Logic 0	0−0.8 V	−0.90 V

ECL is, in fact, used in most modern fast-logic NIM and CAMAC circuits. However, to make them compatible with the NIM standards the levels at the input and output stages are generally adapted. This adds additional cost and power consumption to the module.

ECL modules do away with the adapter stages and enter directly with the ECL levels. This allows a better noise immunity with no loss of bandwidth and minimizes ground loops. Since the input impedance is high (= 100 Ω), cheaper twisted pair cables may be used allowing higher density modules. Flat ribbon cable may also be used but only for short lengths.

NIM signals are not directly compatible with ECL, however, if frequency is not a problem, a very simple translator can be constructed as shown below (Fig. 12.4).

12.5 Analog Signals

Three ranges of analog signals: 0 to 1 V, 0 to 10 V and 0 to 100 V are specified in the NIM convention, however, only 0 to 10 V has found any appreciable usage and indeed almost all commercially available modules work with this definition.

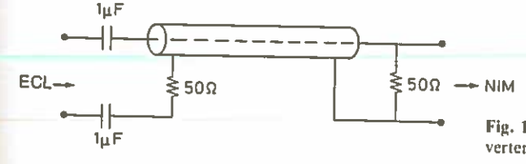

Fig. 12.4. A simple ECL to NIM signal converter (from *Lecroy Catalog* [12.1])

same height and shape. This should be distinguished from the passive pulse splitter discussed in Sect. 14.22.2 which divides both the signal and its amplitude.

The *fan-in*, on the other hand, accepts several input signals and delivers the algebraic sum at the output. These modules may be bipolar, i.e., accepting signals of both polarities, or of single polarity, i.e., accepting signals of one polarity only. Fan-ins are particularly useful for summing the outputs of several detectors or the signals from a large detector with many PM's.

Both fan-ins and fan-outs come in two varieties: linear and logic. The linear modules accept both analog and logic signals, whereas logic fan-outs and -ins are designed for logic signals only. In the case of a logic fan-in, the algebraic sum is replaced by a logical sum (i.e., OR).

14.8 Delay Lines

In making a coincidence measurement, it is important to assure that the electrical paths (and thus the times of propagation) along which two coincident signals travel to the coincidence unit are equal. Delay boxes provide adjustable delays which permit a lengthening or shortening of the electrical paths in a coincidence circuit. The boxes generally consist of variable lengths of cable which in a normal NIM module allow a 0–64 ns delay. Several boxes may be cascaded to give delays of up to a few 100 ns. For longer delays of $\simeq 1\,\mu s$ or more, the length of cable becomes prohibitive and attenuation becomes a factor. In such cases, special low attenuation delay cables must be used or an active electronic circuit.

14.9 Discriminators

The *discriminator* is a device which responds only to input signals with a pulse height greater than a certain threshold value. If this criterion is satisfied, the discriminator responds by issuing a standard logic signal; if not, no response is made. The value of the threshold can usually be adjusted by a helipot or screw on the front panel. As well, an adjustment of the width of the logic signal is usually possible via similar controls.

The most common use of the discriminator is for blocking out low amplitude noise pulses from photomultipliers or other detectors. Good pulses, which should in principle be large enough to trigger the discriminator, are then transformed into logic pulses for further processing by the following electronics (see Fig. 14.14). In this role, the discriminator is essentially a simple analog-to-digital converter.

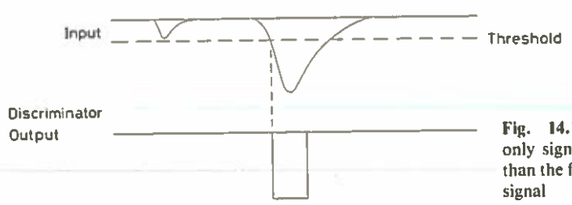

Fig. 14.14. Discriminator operation: only signals whose amplitude is greater than the fixed threshold trigger an output signal

An important aspect of the discriminator is the method of triggering. Because of its use in timing, it is important that the time relation between the arrival of the input pulse and the issuance of the output pulse be constant. In most discriminators, triggering occurs the moment the pulse crosses the threshold level. This is known as *leading edge* (LE) triggering. A more precise method is *constant fraction* (CF) triggering. These techniques are discussed in more detail in Chap. 17.

Two important parameters measuring the speed of the discriminator are the *double pulse* resolution and the *continuous pulse train* or *cw* rate. The double pulse resolution is the smallest time separation between two input pulses for which two separate output pulses will be produced. For fast discriminators, this is usually on the order of a few nanoseconds. The continuous pulse train rate is the highest frequency of equally spaced pulses which can be accepted by the discriminator. This rate can be as high as 200 MHz in fast discriminators.

14.9.1 Shapers

The shaper is a module which accepts pulses of varying width and height and reshapes these pulses into logic signals of standard levels and fixed width. To trigger the shaper, a minimum signal height is required and usually two or more inputs with differing threshold values are provided. Its function is thus identical to that of a discriminator.

The width of the shaper output signals is usually cable-timed, i.e., the width is determined by an external delay cable which the user chooses. In these models, the shaper is bistable so that it may also be operated as a flip-flop. The *set* signal is given at the normal input while the *reset* signal is taken from the *width-in* terminal.

14.10 Single-Channel Analyzer (Differential Discriminator)

The *single channel analyzer* (SCA) or *differential discriminator* (DD) is a device which sorts incoming analog signals according to their amplitudes. Like the discriminator, it contains a lower level threshold below which signals are blocked. In addition, however, there is also an upper level threshold above which signals are rejected. Thus only signals which fall between these two levels provoke a response from the SCA, i.e., a standard logic signal. This is illustrated in Fig. 14.15.

The opening between the upper and lower levels is usually called the *window*. With detectors where the output is proportional to energy, the SCA can be used to measure energy spectra by choosing a small, fixed window and systematically sweeping the window across the full pulse height range. The relative number of counts per unit time at each position can then be plotted to give a histogram of the spectrum.

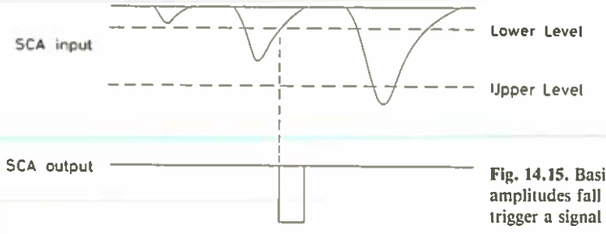

Fig. 14.15. Basic operation of a single channel analyzer (SCA): only signals whose amplitudes fall within the window defined by the upper and lower level threshold trigger a signal

The SCA generally has three working modes, although not all are always available on any given model.

1) Normal Mode or Differential Mode. In this mode, the upper (ULD) and lower (LLD) levels can be adjusted independently of each other, that is the settings of the LLD has no effect on the setting of the ULD and vice-versa. Thus if one wants to select signals with amplitudes between 1 and 2.5 V, for example, the lower level would be set at 1 V and the upper level at 2.5 V. Care should of course be taken to keep the upper level above the lower level.

2) Window Mode. Rather than setting the upper and lower levels separately, in this mode one sets the lower level and the window width, that is the distance between lower and upper levels. In the example above, one would again have the lower level at 1 V, but the *window* (often indicated as ΔE) at 1.5 V ($= 2.5 - 1.0$). This mode has a particular advantage in that the window width is preserved even if the lower level is moved. Thus with $\Delta E = 1.5$ V as above, we could change the LLD to, for example, 3 V, and the ULD would automatically be changed to 4.5 V ($= 3 + 1.5$). This mode is most suitable for spectrum analysis. One can define a certain resolution width, i.e., the window, and sweep this across the range of amplitudes, measuring the relative number of counts at each position without having to change two levels each time.

3) Integral Mode. Here, the upper level is completely removed from the SCA circuit altogether so that one simply has a discriminator with an adjustable lower level. The number of signals which pass is then just the integral of all the pulses from the threshold to the maximum limit of the SCA.

In its role as a pulse height analyzer, the stability and linearity of the SCA threshold becomes an important factor. The degree to which the threshold control and the actual threshold correspond to each other is referred to as *integral linearity*. A typical linearity curve and an ideal curve are shown in Fig. 14.16. In percent, it is defined as

$$L_i = 100 \frac{|\Delta V_{max}|}{V_{max}} \tag{14.1}$$

with L_i: integral linearity; ΔV_{max}: maximum deviation of real threshold from ideal threshold; V_{max}: maximum input voltage to the SCA.

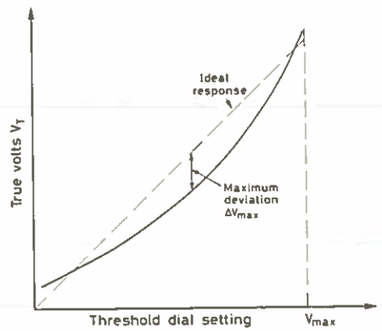

Fig. 14.16. Integral linearity of an SCA (after *Milam* [14.3])

Fig. 14.17. Differential linearity of an SCA (after *Milam* [14.3])

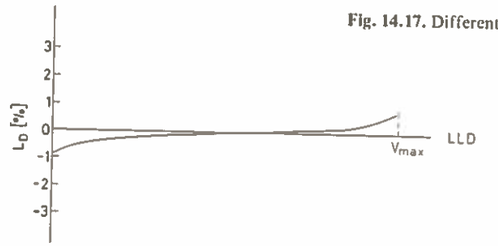

Equally important is the *differential linearity* which gives a measure of the constancy of the window width as the LLD is changed. This is defined as

$$L_d = 100 \frac{\Delta V_w}{V_w} \tag{14.2}$$

with ΔV_w: max. change in window width as LLD is varied; V_w: average window width.

Figure 14.17 shows a plot of typical differential linearity. Clearly it is preferable to work in the middle of the SCA range than at the extremes.

An extension of the normal SCA is the *timing* SCA which also include circuits for correcting *walk* in the generation of the logic signal. The outputs from the SCA's are thus also suited for timing circuits. The various time-pickoff triggering techniques which can be used for this are described in Chap. 17.

14.11 Analog-to-Digital Converters (ADC or A/D)

The ADC is a device which converts the information contained in an analog signal to an equivalent digital form. This instrument is the fundamental link between analog and digital electronics. To give an example of its function, suppose an ADC accepts input pulses in the range of 0 and 10 V and is capable of outputting digital numbers from 0 to a maximum of 1000. (For simplicity, we will use decimal numbers in this example, although in most ADC's this will be expressed in binary form.) An input signal with an amplitude of 2.5 V will thus be converted to the digital number 250. Similarly, for a 150 mV pulse, we would find 15, and so on. The resolution of the ADC depends on the range of digitization. If numbers between 0 and 10000 were generated instead of 0 and 1000, a finer digitization and a higher resolution would be obtained.

ADC's may be of two types: *peak-sensing* or *charge sensitive*. In the former, the maximum of a voltage signal is digitized, as in our example above, while in the latter, it is the total integrated current. The latter is used with current-generating devices, e.g., a PM in current mode (usually fast detectors). Peak-sensing, on the other hand, is used with slower signals which have already been integrated, e.g., a PM in voltage mode. The time of integration or the time period over which the ADC seeks a maximum is usually determined by the width of a gate signal.

Electronically, many methods are in current use for analog to digital conversion. One of the simplest and oldest techniques, often used for spectroscopy ADC's, is the *ramp* or *Wilkinson* method. In this technique, the input signal is first used to charge a

14.14 Time to Amplitude Converters (TAC or TPHC)

The TAC is a unit which converts a time period between two logic pulses into an output pulse whose height is proportional to this duration. This pulse may then be analyzed by a multichannel analyzer to give a spectrum as a function of the time interval. An ADC may also be placed after the TAC to digitize the output pulse. Units such as these are known as *time-to-digital converters* (TDC) and are also found commercially.

A time measurement by the TAC is triggered by a *START* pulse and halted by a *STOP* signal. One simple method used by TAC's is to begin a constant discharge of a capacitor at the arrival of a START signal and to cutoff this discharge when the STOP appears. The total charge collected is then proportional to the time difference between the START and STOP signals. This is illustrated in Fig. 14.22. More on TAC's can be found in Chap. 17.

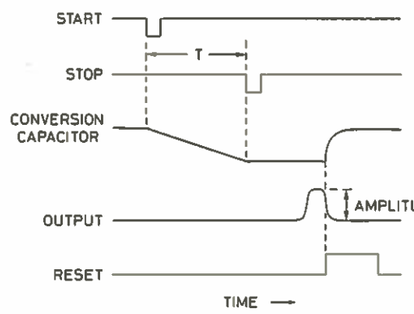

Fig. 14.22. Operation of a time-to-amplitude converter (TAC)

14.15 Scalers

The *scaler* is a unit which counts the number of pulses fed into its input and presents this information on a visual display. So-called *blind* scalers are those which do not have their own integrated display. Their contents may be read by a computer or fed into a separate display unit. In general, scalers require a properly shaped signal in order to function correctly; thus it is usually necessary to have a discriminator or a pulse shaper process signals from the detector before they can be counted by the scaler. Most commercial scalers are also available with a variety of auxiliary functions such as a gate, preset count, reset, etc.

14.16 Ratemeter

The ratemeter is a device which provides the instantaneous average number of events occurring at its input in a given unit of time (i.e. the frequency of events) and outputs this information in the form of a proportional dc voltage level. This output signal can then be used to drive a meter or a chart recorder or both. Like the scaler a standard

logic pulse is usually required at the ratemeter input. A choice of integration times is usually provided as well as a selection of decay constants on the output signal. The latter quantity essentially adjusts the *reaction* time to instantaneous changes in the counting rate.

The ratemeter is a much used instrument appearing mainly in the form of radiation monitors!

14.17 Coincidence Units

The coincidence unit determines if two or more logic signals are coincident in time and generates a logic signal if *true* and no signal if *false*.

The electronic determination of a coincidence between two pulses may be made in a number of ways. One method is to use a transmission gate as we have seen (see Linear Gate). Another simple method often used is to sum the two input pulses and to pass the summed pulse through a discriminator set at a height just below the sum of two logic pulses. This method is shown in Fig. 14.23. Obviously, the sum pulse will only be great enough to trigger the discriminator when the input pulses are sufficiently close in time to overlap. The definition of *coincidence*, here, actually means coincident within a time such that the pulses overlap. This time period determines the *resolving time* of the coincidence and depends on the widths of the signals and the minimum overlap required by the electronics.

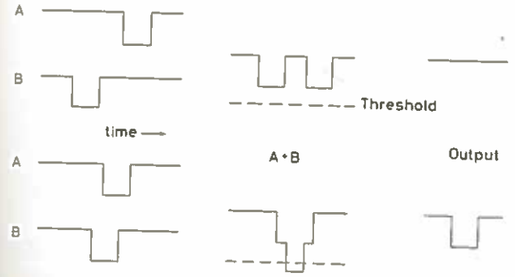

Fig. 14.23. The summing method for determining the coincidence of two signals. The pulses are first summed and then sent through a discriminator set at a level just below twice the logic signal amplitude

The coincidence unit is one example of a more general class of units known as the *logic gate*. These are units which perform the equivalent of Boolean logic operations on the input signals. The coincidence unit, for example, essentially, performs the logical "AND" operation. Other logic gates perform the "OR" operation, "NOT" and combinations of the above. These will be discussed in more detail in Chap. 16.

14.18 Majority Logic Units

A sophisticated and flexible version of the simple logic gates described above is the so-called *majority logic* unit. Such modules accept several input pulses and allow a selection of logical operations on the input. For example, in a majority logic unit which accepts four inputs: A, B, C, and D, one might expect to find the functions shown in Table 14.1.

Table 14.1. Majority logic functions for 4 inputs

Inputs connected	Function	
4	4-fold-AND	$A \cdot B \cdot C \cdot D$
	4-fold OR	$A+B+C+D$
	3-fold majority (any 3 of 4)	$A \cdot B \cdot C+B \cdot C \cdot D+A \cdot C \cdot D+B \cdot A \cdot D$
	2-fold majority (any 2 of 4)	$A \cdot B+A \cdot C+A \cdot D+B \cdot C+C \cdot D+B \cdot D$
3	3-fold AND	$A \cdot B \cdot C$ $B \cdot C \cdot D$ $C \cdot D \cdot A$ $B \cdot A \cdot D$
	3-fold OR	$A+B+C$ $B+C+D$ $A+C+D$ $A+B+D$
	2-fold majority (and 2 of 3)	$A \cdot B+A \cdot C+B \cdot C$ $B \cdot C+B \cdot D+C \cdot D$ $A \cdot C+A \cdot D+C \cdot D$ $A \cdot B+A \cdot D+B \cdot D$
2	2-fold AND	$A \cdot B$ $A \cdot C$ $A \cdot D$ $B \cdot C$ $B \cdot D$ $C \cdot D$
	2-fold OR	$A+B$ $A+C$ $A+D$ $B+C$ $B+D$ $C+D$
1	Pulse shaper	A, B, C, D

14.19 Flip-Flops

The *flip-flop* is a two-input logic device which remains stable in either logic state until changed by an incoming pulse on the appropriate input. Such a device may be formed from two AND gates using feedback loops as shown in Fig. 14.24.

The two input signals are defined as *set* (S) and *reset* (R), while the output signals are Q and its inverse $\bar{Q}$. A *set* signal causes the Q output to go into logic state *1* (and $\bar{Q}$ into *0*), where it will stay until a *reset* signal arrives. The Q output then changes to logic state *0* where it will remain until another *set* arrives, etc. A shortcoming of this device is that the arrival of both a *set* and *reset* at the same time results in an undetermined state. This operation is undefined and it is impossible to predict what will happen. The most likely result is that no reaction whatsoever will occur. This type of flip-flop is known as an SR-flip-flop and is the simplest device of this genre. More sophisticated variants include the JK-flip-flop, the clocked flip-flop, etc. A description of these may be found in any textbook on digital electronics.

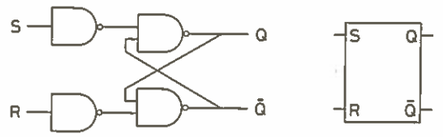

Fig. 14.24. An RS flip-flop and its electronic symbol

The flip-flop is a basic element in digital electronics as it is the only device which essentially *memorizes* the input signal. It may thus be considered as a 1-bit *memory* or *latch*. By combining several flip-flops in parallel, a multi-bit memory for a digital word can then be formed. This is the basis for the register described below. Other uses of flip-flops are illustrated in the following chapters.

14.20 Registers (Latches)

Registers record the pattern of several input pulses (e.g., the signals from an array of counters or the bits of a binary word) and store this pattern in a buffer where it can be read by an external device such as a computer. Most registers are *coincidence* registers requiring the presence of a gate signal in order for the input signals to be recorded.

Registers may also be used to output logic signals. These are known as output registers and are most useful in computer-controlled systems. A bit-pattern written into the register buffer by the computer can then be output as logic signals to control the operation of other devices.

14.21 Gate and Delay Generators

Gate and delay generators or *timers* are triggerable devices which generate variable-width gate pulses ranging from a few nanoseconds to as long as a few seconds. The duration desired is usually chosen by a front panel helipot. Gate generators can be triggered by an input logic signal, and in some cases, manually via a front panel button. The gate pulse then may be used to activate a certain device, for example, a scaler for a chosen length of time. In this way, it serves as a *timer*. These modules are also equipped with an *end marker* signal which is a logic pulse issued at the end of the gate pulse. This feature can then be used as an active logic signal delay. Care, of course, must be taken to ensure the the accuracy of the signal widths and their stability.

14.22 Some Simple and Handy Circuits for Pulse Manipulation

While the NIM standard generally removes most problems of signal compatibility between modules, occasions still arise where some extra manipulation of the pulse signal must be made in order to satisfy some particular condition. Many times the

This circuit is also known as an RC *integrator* as it performs the electrical equivalent of an integration. This can be shown mathematically in the following manner. From Fig. 14.32, we have the equation,

$$V_{in} = iR + V_{out} . \tag{14.14}$$

Substituting,

$$i = \frac{dQ}{dt} = C\frac{dV_{out}}{dt} \tag{14.15}$$

we find

$$V_{in} = RC\frac{dV_{out}}{dt} + V_{out} . \tag{14.16}$$

If $\tau = RC$ is large, then

$$V_{in} \simeq \tau\frac{dV_{out}}{dt} \Rightarrow V_{out} \simeq \frac{1}{\tau}\int V_{in}\,dt . \tag{14.17}$$

If τ is small, however, we have

$$V_{in} \simeq V_{out} . \tag{14.18}$$

Thus in order for the integrator to work, the time constant must be large compared to the pulse. The principal application of the integrator is to smooth out fluctuations in a noisy signal as shown in Fig. 14.33. As a high-frequency filter, however, this integration also affects the fast rise time of the signal. Like the CR differentiator, the RC low-pass filter enjoys an equally important role in pulse shaping in amplifiers.

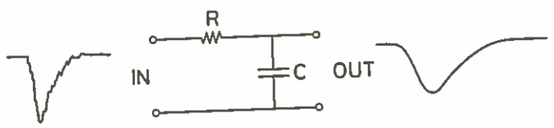

Fig. 14.33. Noise filtering by integration

15. Pulse Height Selection and Coincidence Technique

With this chapter, we begin our discussion of designing and setting up nuclear electronics systems for measurements in nuclear physics. This is a somewhat ambitious goal, as for a given application, there is no one particular system which must be used. Indeed, nowhere does the old adage of "more than one way of skinning a cat" apply more often than here. And if there are any hard and set rules, it is to use lots of imagination! There are nevertheless certain basic systems and methods which have proven their efficiency and efficacy over the years and which provide a foundation for more complex systems. Our method here will be to describe examples of these often used systems using them as illustrations of the how the various functions described in the previous chapter can be combined to give a particular result.

We will begin in this chapter with some simple analog systems and cover two particularly fundamental techniques: setting up and adjusting circuits for pulse height selection and coincidence determination. Once this is understood, the student can go on to the intricacies of electronic logic to which we devote a separate chapter. Before setting up these systems, however, we advise the student to familiarize himself with the use of the oscilloscope, if he has not already. A review of oscilloscope operations is given in Appendix A. A practice to be recommended, in fact, is to examine the input and output signals at each point in the system as it is being set-up. This not only leads to a better understanding of the system, but will also facilitate trouble-shooting later on.

15.1 A Simple Counting System

A basic measurement in nuclear or particle physics experiments is a simple counting of the number of signals from the detector. For example, measuring the activity of a source, or "*plateauing*" a counter. Let us examine a simple electronics set-up for this purpose. Figure 15.1 shows as schematic diagram of the processing units and connections necessary in this system.

In this set-up, the analog signal from the detector is shaped by a preamplifier and amplifier combination. The resulting signal is then sent through a discriminator which delivers a standard logic signal for every analog signal with an amplitude higher than the threshold. The logic signal is then sent to the scaler which counts each arriving

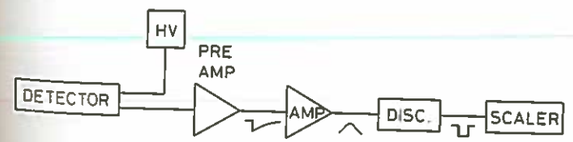

Fig. 15.1. A simple counting system

signal. One should also ensure here that the scaler is of the correct logic type, i.e., it accepts positive (TTL) or negative (NIM) signals, whichever may be the case. NIM to TTL converters may be used if there is an incompatibility.

For some scintillation counters, the direct output is sufficiently large such that amplification is not necessary. In such cases, the detector output may be connected directly to the discriminator.

The discriminator serves the dual purpose of excluding low level electronic noise and shaping the accepted signals to a form acceptable to the scalers. The threshold should be carefully adjusted so as to ensure that electronic noise is eliminated, but not so high as to also cut out good signals.

The scaler should be chosen according to the count rate desired. Evidently, the use of a scaler which is slower than the count rate of the experiment will result in lost counts and bad data! Thus, either take a faster scaler or reduce the count rate.

The system shown in Fig. 15.1 is operated manually, i.e., counting is started and stopped by hand. If two timers, one with a manual trigger, are available, and the scaler is provided with a gate and reset facility, the following circuit may be used for starting and stopping the scaler for fixed time intervals (Fig. 15.2).

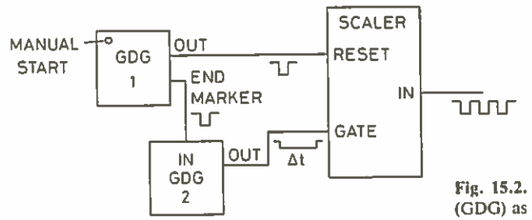

Fig. 15.2. Using two gate and delay generators (GDG) as a timer for a scaler

In this set-up, a short pulse from the first timer, triggered manually, is used to clear the scaler. The end marker then starts a gate pulse which opens the scaler for accumulation for a period equal to the gate width.

15.2 Pulse Height Selection

Often in may experiments, the reaction of interest or the products of the reaction are of a fixed energy or are limited to a small range of energies. For example, in the classic Rutherford scattering experiment, the energy of the probing α-particles is the same before and after scattering. Similarly, in experiments using positron annihilation, the energy of the two annihilation photons is fixed by kinematics. In such measurements, it would, of course, be advantageous to be able to pick out only those events with the correct energies and eliminate the rest. Interference from background reactions would then be reduced and a cleaner, more efficient measurement made. Assuming the use of an energy sensitive detector, such a "*filtering*" can be made by electronically selecting only those signals with the correct pulse height.

A simple system for such a purpose can be formed from Fig. 15.1, by replacing the discriminator with a single channel analyzer (SCA), as shown in Fig. 15.3. This module has adjustable upper (ULD) and lower (LLD) thresholds which define an acceptance "*window*". Pulses with amplitudes falling into this window are accepted and converted

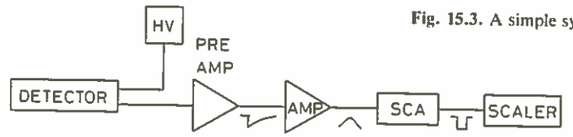

Fig. 15.3. A simple system for pulse height selection

to logic signals while everything else is rejected. The SCA thus acts as a pulse height filter.

In most commercial SCA's, the thresholds are calibrated in volts and are adjustable over the full input range of the module. In slow SCA's this range is usually 0 to 10 V, in accord with the NIM standard for analog signals. For fast SCA's, this is more commonly 0 – 5 V or 0 – 1 V. In either case, both thresholds should remain stable and linear with respect to the dial settings. While this is generally true in the central region, some fall-off may occur near the upper and lower extremes. For this reason, when setting a window, it is advisable to keep it near the center of the input range for the best results. This may require adjusting the gain of the amplifier or detector voltage so that the pulse heights of interest fall into this range.

15.2.1 SCA Calibration and Energy Spectrum Measurement

For energy selection, the thresholds must first be calibrated in terms of energy. In nuclear physics, this can be done by using the SCA to measure the energy spectra of sources with emissions of known energies.

To do this:

1) define a small energy window, $\Delta E = \text{ULD} - \text{LLD}$, for example, 0.1 or 0.05 V.

2) sweep this window across the full input voltage range in non-overlapping steps equal to the window width, and measure the number of counts per unit time at each position. For example, if $\Delta E = 0.10$ V, then starting at 0, measure at positions 0.0 – 0.10, 0.10 – 0.20, 0.20 – 0.30 V, etc. This is a rather tedious operation and is more easily done if the SCA is equipped with a *window* mode of operation; otherwise, the ULD and LLD must be adjusted separately by hand.[1]

3) Plot the results versus LLD setting. A spectrum is thus obtained which should reveal peaks characteristic of the calibration source. A correspondence between LLD and energy can then be made. As an example, Fig. 15.4 shows the spectra from ^{22}Na and ^{60}Co sources taken with a NaI detector using the electronics set-up in Fig. 15.3. A window of 0.05 V was chosen and measurements were made for 10 s at each setting. (As such, the entire measurement took ≈ 1 h!!)

4) Identify the peaks with the aid of the isotope tables. A calibration curve can be drawn by taking the best fitting straight line through the points. This is shown in Fig. 15.4. The energy scale is indicated on the right-hand side of the graph.

One should note the linearity of the calibration. While a minimum of only two points is required to perform the calibration, it is generally a good idea to take more than this number in order to check for any nonlinearities or instabilities in time. Note

[1] When changing the threshold values, be careful of any play in the dial. Turning backwards to a previous position may not be the same as turning forwards to the same position.

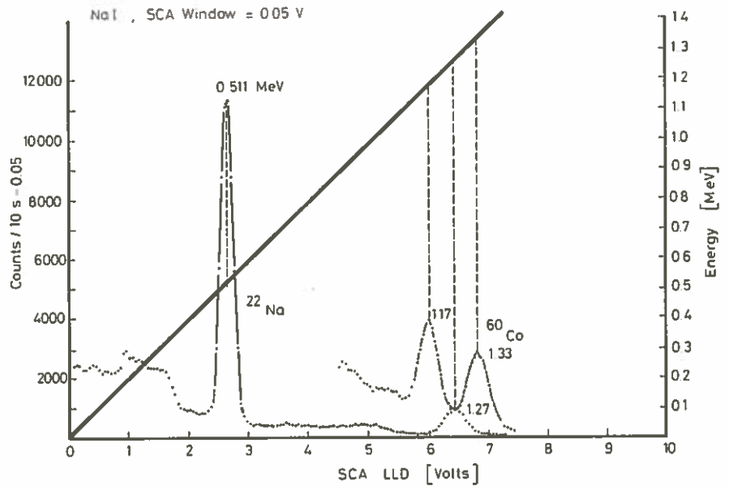

Fig. 15.4. Calibrating an SCA by measuring the pulse height spectrum of known sources. Spectra from ^{22}Na and ^{60}Co are shown along with a calibration line

also that the curve crosses through zero volts at zero energy. If this is not the case, there is most likely a dc offset being added to the signal somewhere in the electronics chain. This is generally not a serious problem as it simply shifts the spectrum to the right or left by a fixed amount.

This calibration is, of course, only valid for a fixed value of the amplifier gain and detector voltage. Changing any of these parameters changes the correspondence between energy and pulse height. In particular, if one follows the recommendation of centering the pulse heights of interest in the input range of the SCA by adjusting the amplifier gain, several calibrations may be necessary. In such a case, a preliminary calibration can first be made with a larger window, for example, and a final more detailed one made when the pulses are centered.

15.2.2 A Note on Calibration Sources

Before ending this section, a word about choosing calibration sources should be made. In general, sources of the same type of radiation as is to be measured in the experiment with energies as close as possible to the desired energy range should be chosen. This is to avoid any possible differences in detector response for different particle types and/or energies. For γ-rays, this is not usually a problem as many γ-ray or x-ray sources covering a relatively large energy range exist. For electrons, however, this becomes somewhat more difficult. The only natural sources of monoenergetic electrons are internal conversion sources and these are generally limited in number and in the range of energies they cover. Moreover, electron detectors are also usually very inefficient for γ-ray absorption by the photoelectric effect, so that the measurement of γ peaks may not be used either. To obtain a wider energy coverage, an alternate method is to measure the energy distribution of electrons coming from the Compton scattering

of γ-rays in the detector. Since the maximum energy of this distribution (the Compton edge) is fixed kinematically and can be calculated from the known energy of the γ-ray (2.110), this point serves as a reference. In this way, the larger variety of γ-sources is also made available for calibration of electron detectors.

When using the Compton edge technique, a problem may arise in determining just where the Compton edge lies. Indeed, the finite resolution of the detector smears out the theoretically vertical edge into a sloping edge so that a sharp structure is no longer available. A common procedure is to choose the mid-point on this slope [15.1]. This appears to work for the Compton edges in Fig. 15.4 if we compare their mid-points to the calibration line. However, some investigators have found the "knee" or peak of the edge or a variable point dependent on energy [15.2] to be better. This can only be determined by trying the various schemes and seeing which gives the most consistent results.

15.3 Pulse Height Spectroscopy with Multichannel Analyzers

In the preceding section, we have described how a pulse height spectrum may be obtained with the use of an SCA. For those who have tried this technique, it is clear that while the method works, it is a tedious operation and not very convenient if many spectra are to be taken. For such work, the multichannel analyzer becomes indispensable. The basic functioning of this device is explained in Chap. 14. Here, we will only discuss some points about the use of the MCA.

Figure 15.5 shows a diagram of the basic set-up. Depending on the ADC and the detectors used, it may be necessary to use a pulse stretcher to shape the signals before entry into the MCA. This is usually the case with fast signals from an organic scintillator. In addition, a biased amplifier can be used if expanded portions of the spectrum are desired. These are optional however and are thus shown in outline in Fig. 15.5.

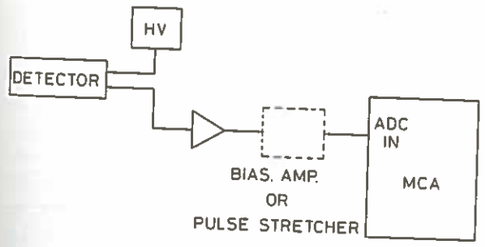

Fig. 15.5. Pulse height spectroscopy with a multichannel analyzer (MCA)

An important factor is the setting of the discriminator. This should not be too high, otherwise, valid portions of the spectrum will be cut out, nor so low as to flood the system with low energy noise. This latter case is a common error by first-time users, but shows up very quickly as an almost 100% dead time on the live-time meter (assuming the MCA is equipped with one!) or with a very high counting rate in the lowest channels.

Even with a correctly set discriminator, attention should be paid to the count rate. If the dead time is greater than 30 – 40%, then this rate is too high. This leads to pulse *pile-up* which results in broaden peaks and a deterioration in resolution. In such cases, the counting rate should be reduced by either increasing the distance between source

several emitted by the source) through an absorber as a function of the velocity of the source relative to the absorber. The source is mounted on a drive which delivers an electronic signal whose amplitude is proportional to velocity. For each transmitted γ-ray, then, we would like to measure this velocity and accumulate the total counts in a MCA. Figure 15.7 illustrates a typical set-up for this purpose.

The velocity signal is sent to the MCA via an amplifier in "*gate*" mode, i.e., a gate signal is required in order for the signal to pass through. At all other times, the signal is blocked. This gate is generated by a signal from an SCA which selects out the correct γ-ray. The spectrum obtained is then transmitted γ's versus source velocity. In place of the gated amplifier, a gated biased amplifier may also be used to allow the expansion of certain portions of the Mössbauer spectrum.

15.4 Basic Coincidence Technique

An extremely important technique in nuclear and particle physics is the electronic determination of coincidences. Like pulse height selection, coincidence in time between two or more events serves as a very powerful criterion for distinguishing reactions.

Figure 15.8 illustrates a simple coincidence measuring system. The basic technique is to convert the analog signal from the detectors into a logic signal and then to send these pulses to a coincidence module. The functioning of such a circuit is described in Sect. 14.17. If the two signals are, in fact, "*coincident*", then a logic signal is produced at the output.

The meaning of *coincident* here deserves some explanation. From the description of the circuit, it can be seen that a coincidence output signal is produced if any part of the

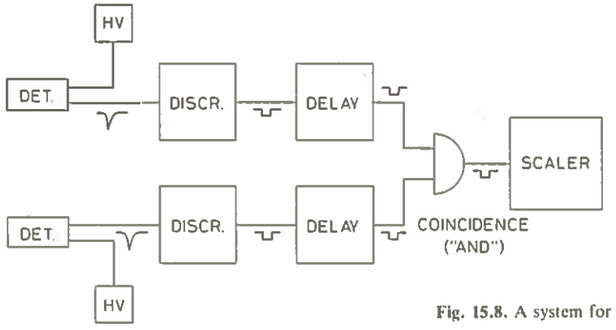

Fig. 15.8. A system for coincidence measurement

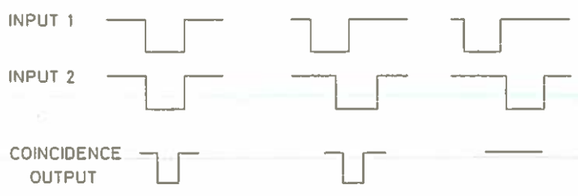

Fig. 15.9. Coincidence between pulses

two incoming signals overlap. (This is the ideal case, of course. In a real circuit, there is generally a minimum overlap necessary before it can be recognized as such. For the purposes of discussion, however, we will consider the coincidence circuit as ideal.) Thus all pulses arriving within a time equal to the sum of their widths are registered as coincident. Figure 15.9 shows some examples of coincident and non-coincident pulses.

In order for this set-up to work, however, it is necessary that the electrical path of each branch leading to the coincidence module be of equal length. This can be ensured by adding adjustable delays to each line, as shown in Fig. 15.8. In principle, only a delay is needed on the faster branch, however, one on each branch provides a bit more flexibility when adjusting the circuit.

15.4.1 Adjusting the Delays. The Coincidence Curve

To adjust the delays, a source of true coincident events is necessary. For γ-ray detectors a very common source is radiation from positron annihilation (e.g. ^{22}Na). Here, two photons of equal energy are emitted in opposite directions. If the detectors are placed face to face with the annihilation source between them, then these events may be used to adjust the delays.

If the detectors are inefficient for γ-ray detection but are thin, for example, plastic scintillators, coincidences may be obtained by placing the detectors close together and allowing a beam of charged particles (from a β source, for example) to pass through both counters. Be sure the particles have sufficient energy to penetrate through the counters, however! These two set-ups are illustrated in Fig. 15.10 and should be applicable most of the time. However, there will, of course, be situations in which neither of the above is suitable. In such cases, some imagination must be used!

With a source of coincident events, the relative values of the delays can be found by measuring the number of coincidences as a function of delay setting. Plotting the results on a graph gives what is then known as the *coincidence curve.* This is illustrated in Fig. 15.11.

Here we have plotted the delay setting of branch 1 on the positive x-axis and the delay of branch 2 on the negative x-axis since this represents a negative delay of branch 1 relative to branch 2. It should be noted that even with a zero delay setting on the box, a certain delay ($\simeq$ a fraction of a ns) is still present just from passing through the box. In our set-up with delay boxes on both branches, this is equalized. However, if only one

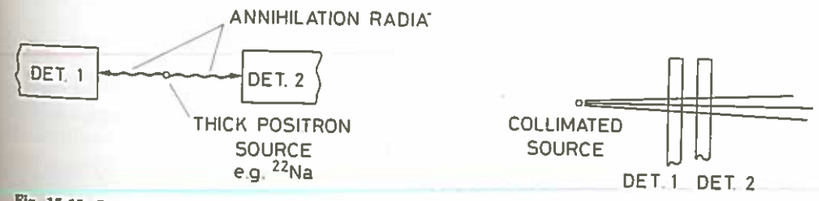

Fig. 15.10. Set-up for adjusting the coincidence between two detectors. For gamma ray detectors, the two photons from positron annihilation provide a useful source of coincident events. For charged particle detectors, a beam of electrons or other particles may be used provided the particle energy is high enough (and the counters thin enough) for the particles to pass through at least the first counter

Fig. 15.11. A measured coincidence curve

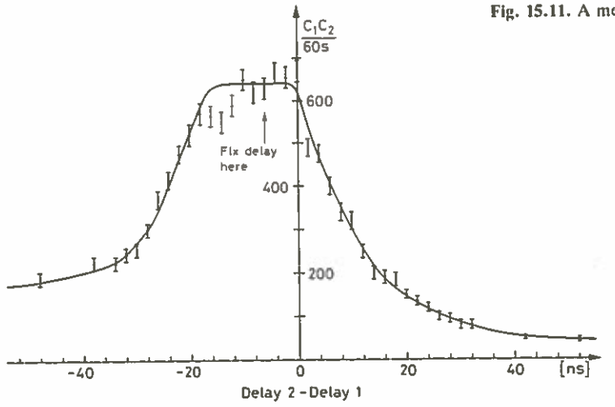

box is used and the coincidence curve is made by placing the box on one branch and then the other, the *zero* points of each branch will *not* coincide because of this residual delay!

From this curve, it is clear that the correct setting for the delay is that in the middle of the plateau. Ideally, of course, this coincidence curve should be perfectly rectangular in shape as it, in principle, corresponds to the region of overlap between the two rectangular pulses. However, timing variations arising from the detectors and the electronics (as well as the less than perfect shape of the signals) cause a *jitter* in the time relation between the two signals which smears out the sides of the curve. If the width of the signals is smaller than these fluctuations true coincidences will, in fact, be lost. Measurements of the coincidence curve will therefore fluctuate giving the curve an aberrant shape. In such a case, the widths should be enlarged so as to encompass this *time jitter*. These effects are the limiting factors in a coincidence circuit and are discussed in more detail in Chap. 17.

The full width of this curve at half its maximum height (FWHM) is usually taken as the *resolving time* of the system. This time should generally be close to the sum of the two pulse widths. Obviously, the narrower this curve, the better is the capability of the circuit for distinguishing small time intervals and the less accidental coincidences. To increase this resolution, one might at first be tempted to decreases the widths of the pulses to the minimum. However, this is limited by the timing fluctuations which we have mentioned.

15.4.2 Adjusting Delays with the Oscilloscope

While not as precise as measuring a coincidence curve, a quick method of finding the approximate delay settings is to view the two pulses on a dual trace oscilloscope. By triggering on one pulse, the time relation of the second may be seen quite readily and appropriate delays can be added or subtracted to bring the pulses into an overlap condition. In doing this, of course, one should also ensure that the cable leads to the oscilloscope are both of the same length! Figure 15.12 illustrates this technique.

While this method is quite convenient, it requires a relatively intense source of coincidences, (especially when inefficient detectors are involved), in order for the second

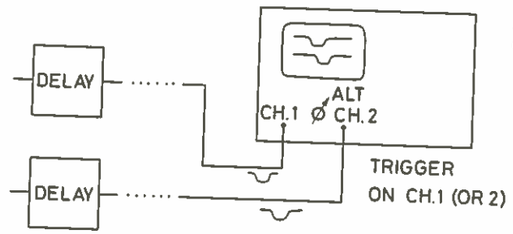

Fig. 15.12. Adjusting a coincidence circuit with the oscilloscope

signal to have sufficient intensity to be seen clearly on the oscilloscope screen. In the case of a weak signal, one must resort to measuring a coincidence curve.

15.4.3 Accidental Coincidences

In making a coincidence measurement, one must also consider the possibility of *accidental* coincidences occurring in the circuit. These may be due to uncorrelated background events in the detectors which happen to arrive within the resolving time of the circuit or to random noise which triggers the discriminators, etc. Clearly in any measurement, the number of such accidentals must be kept to a minimum.

The rate of accidentals in any coincidence setup may be estimated from the singles rate in each branch and the time resolution of the system. Suppose N_1 and N_2 are the singles counting rates for branches 1 and 2 respectively and σ is the resolution. Since any overlap in these pulses produces a coincidence, this means that the signals need only be within a period σ of each other in order to trigger the module. Assuming a constant singles rate, then, for each signal which arrives from branch 1, there will be $N_2\sigma$ pulses from branch 2 which fall into this allowable time period. Since there are N_1 pulses/unit time in branch 1, the total number of accidentals per unit time will be

$$\text{Accidentals} \simeq \sigma N_1 N_2 . \tag{15.7}$$

This rate may also be measured, and, in fact, corresponds to the baseline of the coincidence curve in Fig. 15.11. This automatically suggests a method for measuring the accidentals simultaneously with the true coincidences, i.e., form a second coincidence circuit with delays set so as to be completely off the coincidence curve. With current NIM modules which contain multiple outputs and multiple coincidence circuits within one physical module, such side measurements are facilitated.

15.5 Combining Pulse Height Selection and Coincidence Determination. The Fast-Slow Circuit

We have seen now how to set-up a system for pulse-height selection and a circuit for coincidence determination. The next obvious step is to consider combining the two. One way would be the set-up illustrated in Fig. 15.13.

The signals from the detectors are amplified and shaped, then sent to *timing SCA's* for pulse height testing. The logic pulses from these modules are corrected for *walk*

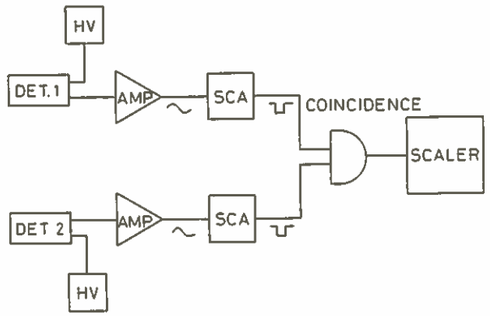

Fig. 15.13. A system with pulse height selection and slow coincidence

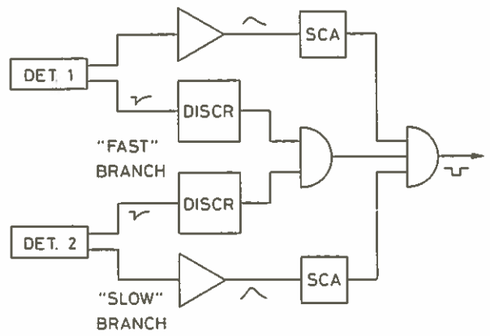

Fig. 15.14. A *fast-slow* coincidence system

effects (see Chap. 17) and may be tested for coincidence. Such a system generally gives good timing resolution and is adequate for most purposes.

It is clear, however, that in such a system the shaping of the pulse destroys some of the rise time information and does not represent the ideal situation for timing even with walk correction. Indeed, if the maximum in timing and pulse height resolution is desired, a so-called *fast-slow* system can be used. Such a system divides the signal into two branches, fast and slow, treates each separately and then combines the results. This system is schematically outlined in Fig. 15.14.

The *slow* branch is sent to a shaping amplifier and tested for pulse height in the usual manner. The *fast* branch, on the other hand, is passed directly (or through a fast amplifier) into a fast coincidence. This signal is then placed in a triple-fold coincidence with the slow branch. In this way, the cirteria of a fast coincidence is added to the slower coincidence of the SCA signals.

With scintillation counters, a method that is sometimes used is to take the slow signal from one of the later PM dynodes and the fast signal from the normal anode. The dynode signal is somewhat more linear since it is less saturated, while the anode signal has less time jitter because of its greater amplitude.

For fast scintillator signals, a recent development has been the construction of fast SCA's which allow both a fast timing signal and a good pulse height selection on unshaped signals. With such modules, the simpler set-up in Fig. 15.13 may then be used.

15.6 Pulse Shape Discrimination

In addition to pulse height information, the signals from some detectors also carry information in their shapes, (or more precisely in their rise and decay times). A prime example is the liquid scintillator NE213 which has the characteristic of emitting different pulse shapes in response to different types of particles. This is a result of the different ionizing powers of the particles which give rise to different excitation mechanisms in the scintillator and in consequence, different fluorescent decay times (see Sect. 7.2). A similar effect may be found in large ionization detectors. Particles of differing ionization power produce longer or shorter ionization trails in the detector volume which result in different charge collection times and hence different pulse shapes at the

detector output. The technique of pulse shape discrimination (PSD) takes advantage of this property to allow a distinction between particle types when different incident radiations are present. One of the most common applications of PSD in in fast neutron detection where large gamma-ray backgrounds often accompany the neutrons. Using PSD, the gamma ray events may be selected out and suppressed leaving only the neutrons or vice versa.

Electronically, discriminating between different pulse shapes requires measuring the decay time of each pulse and this independently of the amplitude. In practice, this can be done efficiently only over a limited range of amplitudes (the *dynamic range*), which, for some applications such as spectroscopy, may imply certain restrictions. A second consideration is the speed of the PSD circuit. For high count rates, this becomes an important limiting factor. Not surprisingly therefore, a number of different circuits have been developed over the years. One of the most widely used methods is the *zero-crossing* system [15.3] shown in Fig. 15.15. This method offers a wide dynamic range and is relatively easy to implement; it is, however, limited to maximum count rates on the order of 20 – 30000 counts/s.

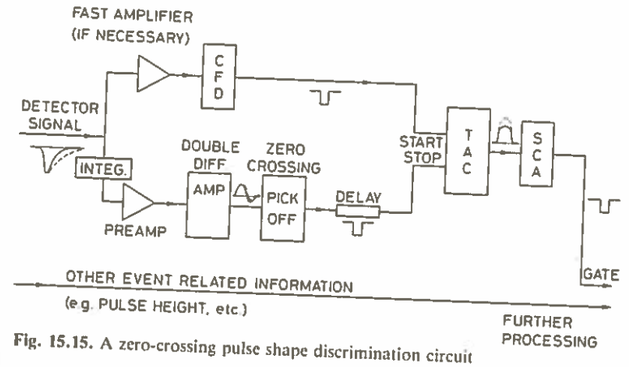

Fig. 15.15. A zero-crossing pulse shape discrimination circuit

In this system, the detector output signal is first split into two with one branch going to a fast time-pickoff discriminator (a constant fraction, for example), which triggers on the fast leading edge of the signal and starts a TAC or some other type of timing circuit. The second branch is integrated and sent through a preamplifier. This results in a pulse whose rise time depends on the decay time of the initial pulse (see, for example, Fig. 7.12). This signal is then doubly differentiated by a double delay amplifier which produces a bipolar pulse whose zero-crossing time depends on the input rise time. A zero cross-over pickoff module now triggers on this point and generates a STOP signal for the TAC. The time period measured by the TAC is thus proportional to the decay time of the detector pulse. Figure 15.16 shows a typical TAC spectrum from an NE213 detector in a field of neutrons and gammas. The two types of particles are clearly distinguished. To select a particular particle, an amplitude selection is performed on the TAC signal using an adjustable discriminator of SCA. The resulting logic signal may then be used to gate a recording instrument such as an MCA. Alternatively, the TAC pulse may be digitized and selected by computer, or stored on some sort of recording medium along with other event related information for analysis at a later time.

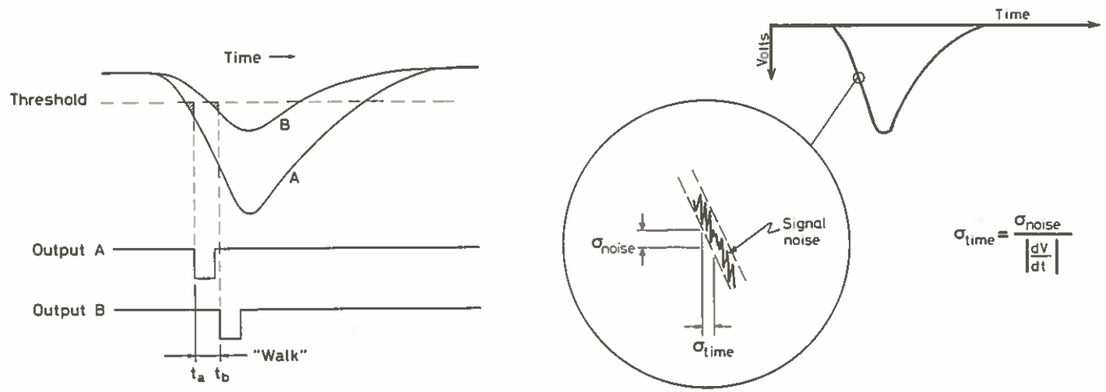

▲
Fig. 17.1. *Walk* in a discriminator or SCA. Coincident signals with different amplitudes cross the threshold at different times. An additional *walk* effect occurs because of the finite charge which must be integrated on a capacitor to trigger the discriminator or SCA

Fig. 17.2. Timing jitter. The timing error caused by jitter depends on the slope of the signal at the triggering point

In PM systems, for example, jitter is influenced by factors such as: (1) variations in the number of photons created in the scintillator, (2) the transit time of the photons and the electrons through the scintillator and PM, (3) gain variations in the electron multiplier, etc. Unlike walk, therefore, jitter arises from the intrinsic detection process itself. The effect of noise and statistical fluctuations on the timing resolution is easily calculated from Fig. 17.2. If σ_n is the variance in V due to noise and statistics, projecting this region onto the horizontal time scale yields the rms fluctuation in time,

$$\sigma_{time} = \frac{\sigma_n}{\left|\frac{dV}{dt}\right|} \,. \tag{17.1}$$

Thus the rms timing resolution depends inversely on the slope of the signal – the faster the risetime, the better the timing jitter. In detectors with variable risetimes such as semiconductors or ionization instruments, this also suggests setting the triggering threshold at the point of greatest risetime to obtain the best results.

17.2 Time-Pickoff Methods

17.2.1 Leading Edge Triggering (LE)

The simplest method for deriving a timing logic signal is *leading-edge* (LE) triggering. This is the technique illustrated in Fig. 17.1 and, as we have seen, the logic signal is generated at the moment the analog pulse crosses the threshold. In SCA's this signal is generally delayed until the maximum of the pulse signal is first tested. An alternate method also used in some cases is to trigger on the falling edge.

This method is inherently subject to problems of walk, but can be used with good results if the amplitudes are restricted to a small range. With a 1 to 1.2 amplitude range, for example, resolutions as low as ≃0.4 ns can be obtained with a well-designed system of fast organic scintillators. At a 1 to 10 range, however, the walk effect balloons to as much as ±10 ns.

Walk can also be minimized by using as low a threshold as permitted by the electronic noise. This is easily verified by lowering the threshold line in Fig. 17.1. In low noise systems, the leading edge may even be amplified, so as to get closer to the beginning of the signal. However, noise jitter is then increased as given by (17.1).

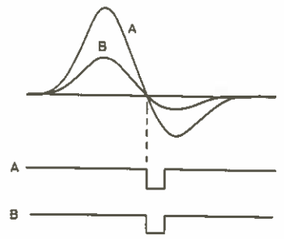

Fig. 17.3. Zero-crossing timing. Variations in the cross-over point are known as *zero-crossing walk*

17.2.2 Fast Zero-Crossing Triggering

The *fast zero-crossing* technique was developed mainly to overcome the walk problem inherent in the LE method. Here, the pulse is first transformed into a bipolar pulse (through double delay line shaping, for example) and the trigger made on the zero-crossing point of the resulting bipolar pulse. This is illustrated in Fig. 17.3 which shows two pulses of differing amplitudes after being doubly differentiated. As can be seen, the two crossing points are precisely related in time and independent of the pulse amplitudes. As with LE timing, a maximum resolution of ≃0.4 ns is obtained if the amplitude range is restricted to 1 : 1.2; however, at 1 : 10, this maximum resolution only increases to ≃0.6 ns, an enormous improvement! Unfortunately, this method requires that the signals be of constant shape and rise-time. It is thus unsuited for signals from large volume semiconductor detectors or very large scintillators where such variations may occur.

17.2.3 Constant Fraction Triggering (CFT)

Probably the most efficient and versatile method available today is the constant fraction triggering technique. In this method, the logic signal is generated at a constant fraction of the peak height to produce an essentially walk-free timing signal. The basis for this idea arose from empirical tests which showed the existence of an optimum triggering level [17.1] for the best timing resolution. Depending on the type of signal, this level occurs at a certain fraction of the pulse height independent of the amplitude. Figure 17.4 shows how this works at a constant fraction of 50%.

The technique by which *CF* triggering is achieved is illustrated in Fig. 17.5. The incoming pulse V_a is first split into two with one part (V_d) delayed by a time τ_d equal to the time it takes for the pulse to rise from the constant fraction level to the pulse peak. The other part is inverted and attenuated by a factor k to give a pulse $V_c = -kV_a$. The two are then summed to produce a bipolar pulse, V_{out}. The point at which the signals cancel, i.e., the zero-crossing point, is then at a constant fraction k of the original signal height.

Unlike the zero cross-over technique, the CFT method does not require a bipolar pulse at the input, however, a constant rise-time is necessary. The efficiency of this technique is, nevertheless, very high yielding walk of as little as ±20 ps over an amplitude range of 100 to 1.

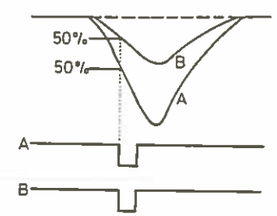

Fig. 17.4. Constant fraction discrimination

17.2.4 Amplitude and Risetime Compensated Triggering (ARC)

As we have seen, the constant fraction method produces an essentially walk-free signal but requires that all pulses have the same rise time. This latter requirement can be re-

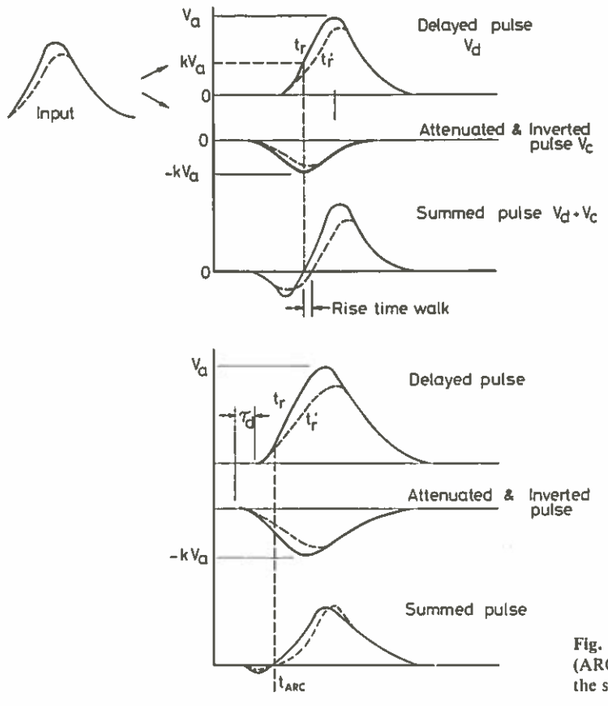

Fig. 17.5. Technique for constant fraction triggering. In order for this technique to work rise times of all signals must be the same. The dotted line shows the result with a different rise time signal

Fig. 17.6. Amplitude and risetime compensation (ARC) triggering. The zero-crossover occurs before the signal peak is reached

moved with a variant of CFT known as *amplitude and risetime compensation* (ARC) triggering. The difference is simply in the delay τ_d. In the true CFT method, τ_d must be long enough to allow the undelayed signal to reach its peak. In the ARC method, τ_d is made smaller than the rise time so that the summed signal crosses before the signal maximum is reached. The zero-crossing time thus depends only on the early portion of the signal where differences between pulse shapes are at a minimum. This is illustrated in Fig. 17.6. ARC triggering is the most precise method available today and is most useful with large volume semiconductor detectors where the pulses vary in shape as well as amplitude.

17.3 Analog Timing Methods

Assuming that the proper choice of time-pickoff method is chosen, let us now consider some electronic techniques for measuring the time difference between two signals. We divide these into analogic and digital techniques.

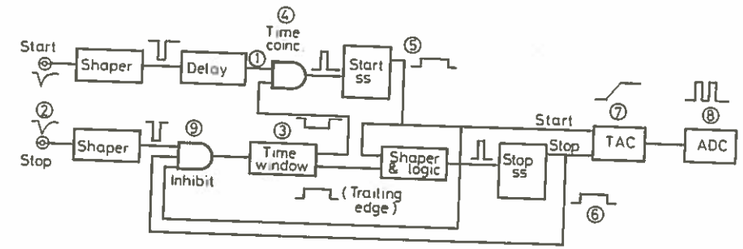

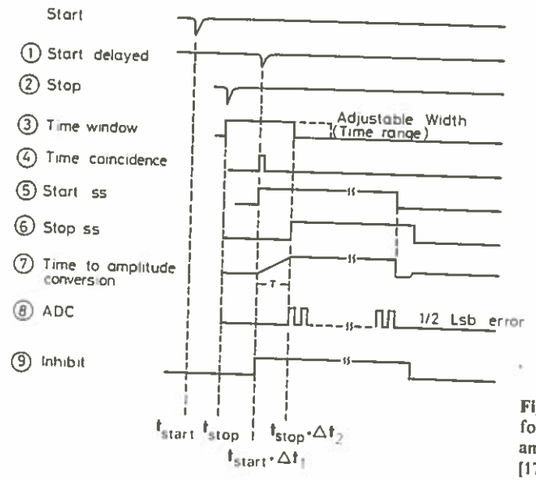

Fig. 17.7. Logic and timing diagrams for a START-READY-STOP time-to-amplitude converter (from *Porat* [17.2]; picture © 1973 IEEE)

17.3.1 The START-STOP Time-to-Amplitude Converter

The primary example of analogic time interval measurement is the START-STOP time-to-amplitude converter. The basic method is to relate the time interval between two events to the quantity of charge discharged by a capacitor during this period. As shown in Fig. 14.22, the arrival of the first signal (START) gates on the capacitor which discharges at a constant rate until the arrival of the STOP signal. The total charge collected thus forms an output signal whose height is proportional to the time difference between the START and STOP signals. The capacitor is then recharged and the next event awaited. If no STOP signal arrives, however, the output signal reaches its maximum amplitude which then causes an overflow condition. Such events, of course, cause a great deal of dead time. To remedy this, some START-STOP TAC's include additional logic circuits at the beginning to test for the presence of a STOP within the allowed time window before discharging of the capacitor begins. This technique, sometimes known as START-READY-STOP, is illustrated in Fig. 17.7.

Referring to the timing diagram, an arriving START signal is first shaped and delayed by a period Δt_1 equal to the time window. When a STOP pulse arrives, a time window signal of width $\Delta t_2 (= \Delta t_1)$ is generated which is then tested for coincidence with the delayed START. It is easy to see, now, that this coincidence is TRUE if the STOP has arrived within the time window and FALSE otherwise. In this manner, bad